Synthesis of Branched Polyethylene Using (α-Diimine)nickel(II) Catalysts: Influence of Temperature, Ethylene Pressure, and Ligand Structure on Polymer Properties

Derek P. Gates, Steven A. Svejda, Enrique Oñate, Christopher M. Killian, Lynda K. Johnson, Peter S. White, and Maurice Brookhart*

Department of Chemistry, University of North Carolina at Chapel Hill, Chapel Hill, North Carolina, 27599-3290

Received July 27, 1999; Revised Manuscript Received December 13, 1999

ABSTRACT: Detailed investigations of the polymerization of ethylene by (α-diimine)nickel(II) catalysts are reported. Effects of structural variations of the diimine ligand on catalyst activities, polymer molecular weights, and polymer microstructure are described. The precatalysts employed were [{(2,6-RR′C_6H_3)−N═C(Nap)−C(Nap)═N−2,6-RR′C_6H_3)}$NiBr_2$] (Nap = 1,8-naphthdiyl) (**4a**, R = CF_3, R′ = H; **4b**, R = CF_3, R′ = CH_3; **4c**, R = C_6F_5, R′ = H, **4c**, R = C_6F_5, R′ = H; **4d**, R = C_6F_5, R′ = CH_3; **4e**, R = CH_3, R′ = H, **4f**, R = R′ = CH_3; **4g**, R = R′ = $CH(CH_3)_2$), [{(2,6-C_6H_3(*i*-Pr)$_2$)−N═C($CH_2CH_2CH_2CH_2$)C═N−(2,6-C_6H_3(*i*-Pr)$_2$)}$NiBr_2$] (**5**), and [{(2,6-C_6H_3(*i*-Pr)$_2$)−N═C(Et)C(Me)═N−(2,6-C_6H_3(*i*-Pr)$_2$)}$NiBr_2$] (**6**). Active polymerization catalysts were formed in situ by combination of **4**−**6** with modified methylaluminoxane. In general, as the bulk and number of *ortho* substituents increase, polymer molecular weights, turnover frequencies and extent of branching in the homopolyethylenes all increase. Effects of varying ethylene pressure and temperature on polymerizations are also reported. The degree of branching in the polymers rapidly decreases with increasing ethylene pressure but molecular weights are not markedly affected. Temperature increases result in more extensive branching and moderate reductions in molecular weights. Catalyst productivity decreases above 60 °C due to catalyst deactivation.

Introduction

The development of well-defined early-transition-metal- and lanthanide-based catalysts for the polymerization of ethylene and α-olefins has been the subject of intense recent study.[1] These homogeneous catalysts represent a significant technological advance over traditional heterogeneous Ziegler−Natta systems in that insight into mechanisms of polymerization can be gained, and rational changes to the catalyst structure can be used to control polymer microstructure and properties. Although early metal catalysts currently dominate industrial polymerization processes, there has been a trend toward the development of catalysts containing late-transition-metal elements. Relative to early-transition-metal catalysts, these systems have the potential to yield polymers with different microstructures and should be less oxophilic and therefore more tolerant of functionalized monomers. Currently, well-defined catalysts based on complexes of cobalt,[2−4] rhodium,[5,6] nickel,[7−24] palladium,[8,25,26] platinum,[6] and iron[27−29] have been reported to polymerize olefins.

A major focus of our work has involved the development of olefin polymerization catalysts based upon cationic α-diimine complexes of nickel and palladium of general structure **I**, the first report of which appeared in 1995.[8,9] Alternatively, active catalysts may be readily generated and used in situ by reaction of dibromide **II** with methylaluminoxane (MAO). Subsequently, other groups have reported olefin polymerizations using identical or closely related catalyst systems.[17,19−23] These catalysts polymerize ethylene and α-olefins to high molecular mass polymer with activities of the nickel(II) system comparable to early-transition-metal systems. Dramatic differences in the microstructure and properties of polymers made using these nickel- and palladium-based catalysts are observed as compared to polymers made using early metal Ziegler−Natta and metallocene technology. For example, branching in polyethylene prepared with nickel(II)- or palladium(II)-based catalysts can vary from highly branched to linear, and the properties thus vary from soft elastomers to rigid plastics, respectively. The polymer properties observed are greatly dependent on reaction conditions, ligand structure, and the metal. For example, catalysts lacking bulky substituents in the *ortho* aryl positions have been found to oligomerize ethylene selectively to α-olefins.[11,12] Furthermore, bulky nickel(II) catalysts have been shown to catalyze the living polymerization of α-olefins (i.e., propylene, 1-hexene, etc.) at −10 °C, and thus provide access to diblock and multiblock copolymers.[10] Palladium-based catalysts have proven to be tolerant of certain functional groups and will copolymerize alkyl acrylates with ethylene and α-olefins.[25,26] Recently, internal olefins such as cyclopentene have been polymerized with both nickel- and palladium-based catalysts, forming a unique high molecular weight poly(cyclopentene) with 1,3-enchainment via an addition mechanism rather than the expected 1,2-enchainment.[13,30]

A general mechanism for the polymerization has been proposed and is shown in Scheme 2. The catalyst resting state for the Pd(II) systems is the alkyl olefin complex **A** as established by ^{1}H NMR spectroscopy.[8,31] The same resting state applies in the Ni(II) systems at low temperature.[32] The turnover-limiting step is the migratory insertion reaction to yield an intermediate cationic alkyl complex **B**. This species has been shown to be a *β*-agostic species in the Pd(II) systems,[13,31] but for simplicity is shown in Scheme 2 without the M−*β*-H−C interaction. Metal migration (chain running) along the alkyl chain can occur in these species via *β*-H elimination/readdition reactions (to **C** and **D**) as shown in

10.1021/ma991234+ CCC: $19.00
Published on Web 03/08/2000

Scheme 1. (α-Diimine)−Ni(II) and −Pd(II) Olefin Polymerization Catalysts/Catalyst Precursors

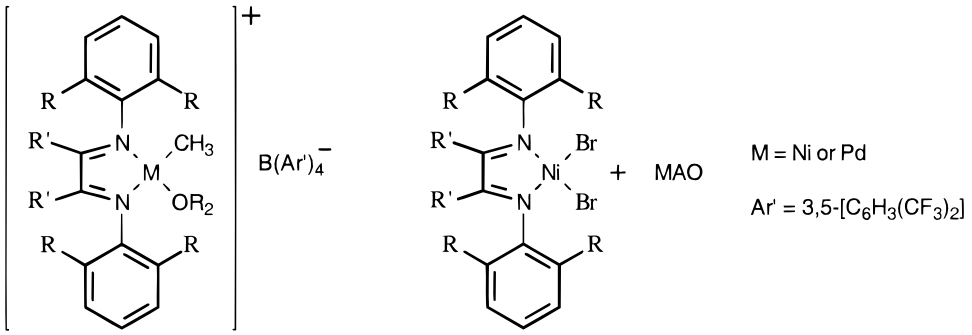

I **II**

Scheme 2. Proposed Mechanism of Propagation for the Preparation of Branched Polyethylene Using Ni(II) Catalysts

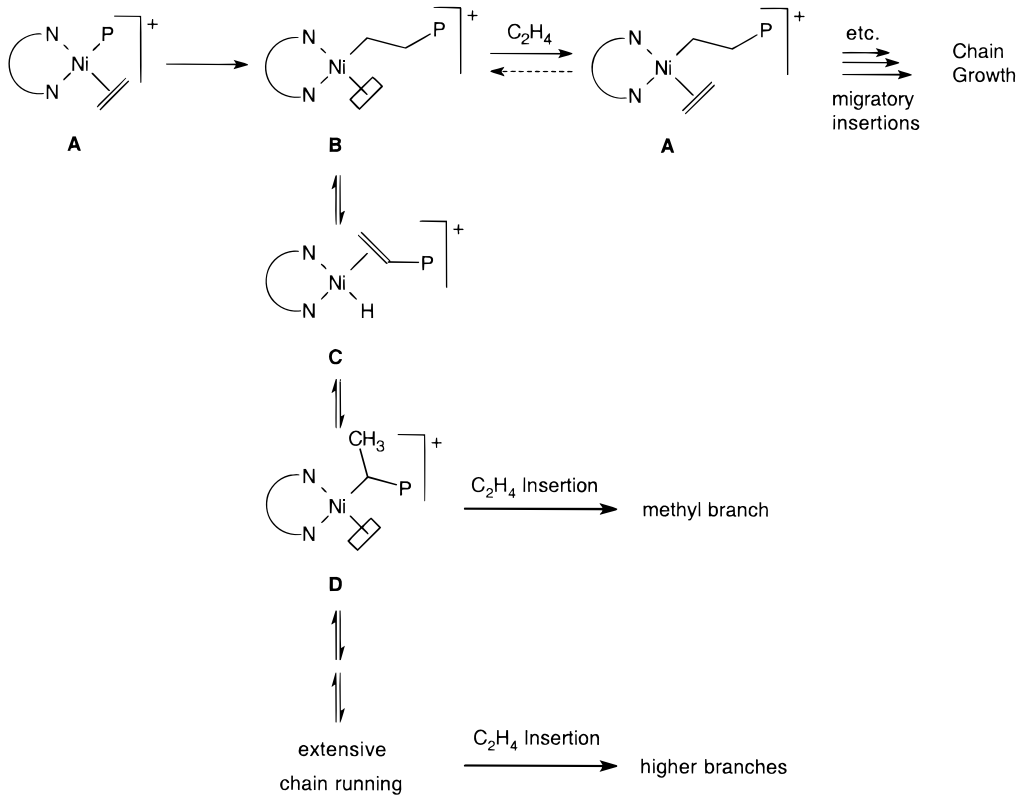

Scheme 2.[8,9,26,31] (A similar proposal was made by Fink to account for structures of 1-hexene oligomers from certain Ni(II) catalysts.)[14,15] These migration reactions occur without chain transfer. Successive migratory insertion and ethylene trapping cycles from **A** leads to a linear polymer. Insertion following chain running leads to the introduction of branches in the polymer chain. The greater the extent of chain running prior to insertion the more highly branched the polymer.[8,9,33] In the case of nickel, trapping and insertion are competitive with chain running, and thus the extent of branching is sensitive to ethylene pressure, decreasing with increasing ethylene pressure.

A critical feature of these catalysts is that, unlike most late metal systems, the rate of chain transfer (k_{ct}) is much slower than the rate of propagation (k_p), and thus a high polymer results from polymerization of ethylene and α-olefins. The key feature leading to slow chain transfer is the presence of bulky *ortho* aryl substituents which are situated above and below the axial positions of the square planar complex. Generally, the more sterically encumbering the substituents, the higher the polymer molecular weights (i.e., the greater k_p/k_{ct}). Initially, the slow rate of chain transfer was ascribed to a slow associative displacement of the unsaturated polymer chain as a result of the bulky *ortho* substituents blocking axial approach of the monomer (see Scheme 3). Recent calculations by Ziegler et. al. have suggested that chain transfer occurs by direct β-H transfer to monomer in the alkylolefin resting state **A** and that this barrier increases with increasing steric bulk of the *ortho* substituents.[34,35] Currently, no firm experimental evidence is available which distinguishes these mechanisms. Several other theoretical analyses of these systems have appeared which agree in large measure with the mechanistic details derived from our experimental studies.[36,37]

In this paper, as a followup to our initial communication,[8] we report on our detailed investigations of the polymerization of ethylene using (α-diimine)nickel(II)

Scheme 3. Proposed Mechanism of Chain Transfer

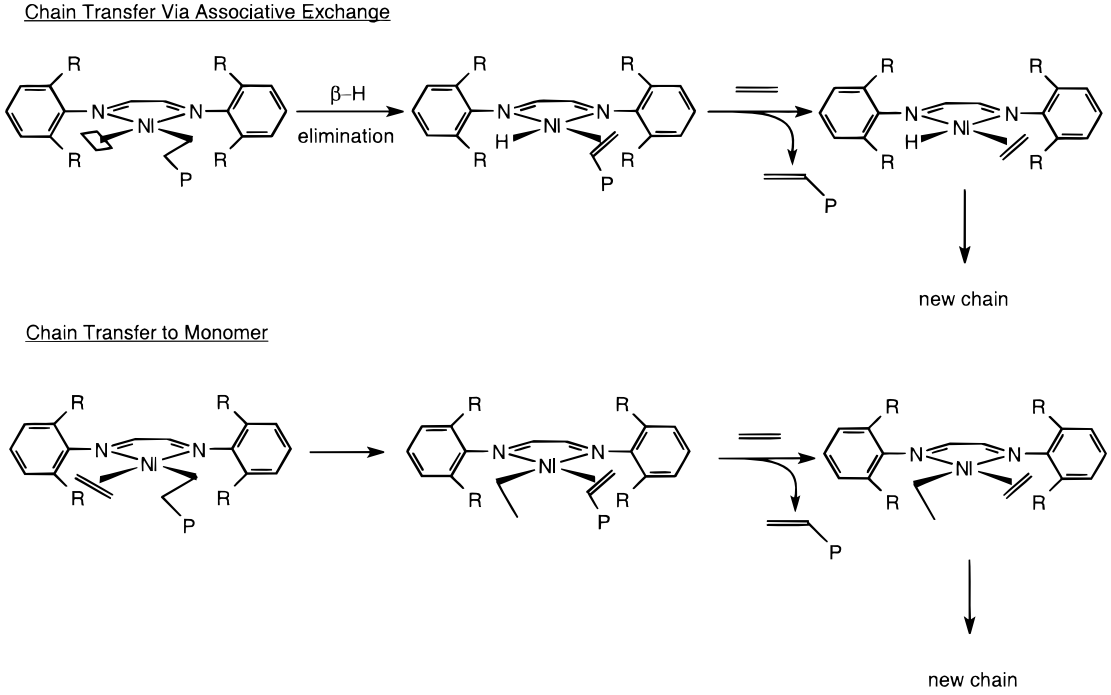

Scheme 4

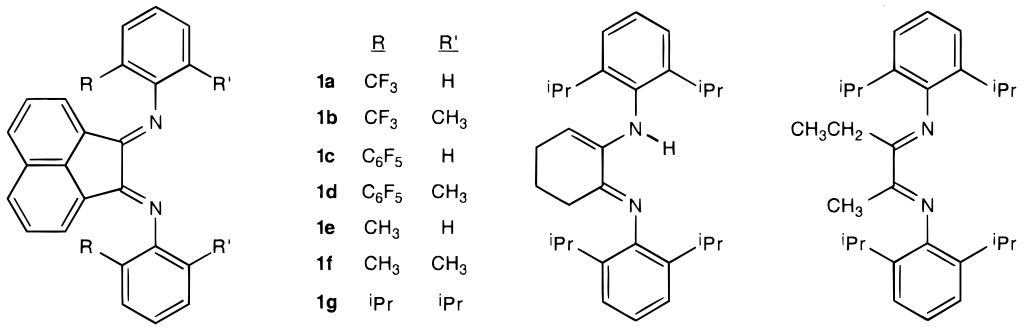

Scheme 5

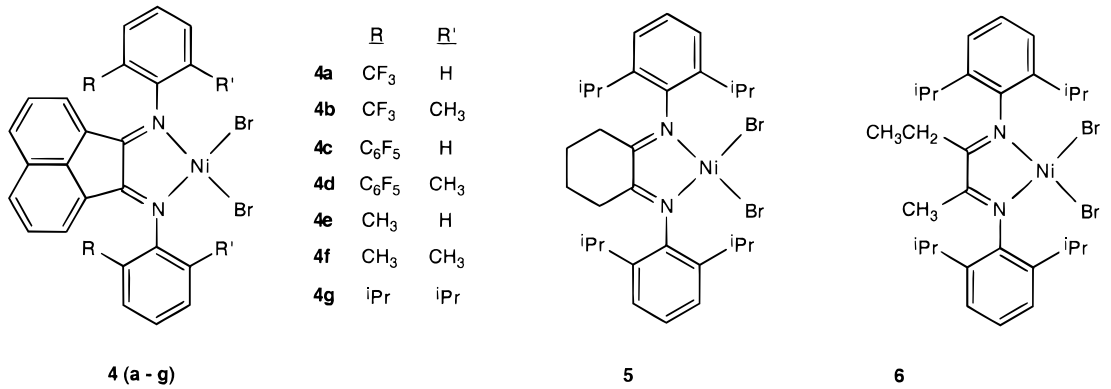

catalysts. To gain more insight into the factors controlling the activity of the catalysts and the effect of catalyst structure on polymer structure and properties, we have examined several aryl-substituted α-diimine systems with variable *ortho* substituents including isopropyl, methyl, trifluoromethyl, and pentafluorophenyl groups as well as variations in substitution at the backbone carbon atoms of the α-diimine ligand. The effect of temperature and ethylene pressure on activity and polymer microstructure, and the effect of catalyst structure on chain transfer and catalyst lifetime will also be presented.

Results and Discussion

A. Synthesis of α-Diimine Ligands and Corresponding Nickel(II) Bromide Complexes. The α-diimine ligands and the corresponding nickel(II) dibromide complexes prepared for study are summarized in

Schemes 4 and 5, respectively. Compounds **1e**−**g** are known,[38] and certain aspects of the polymerization behavior of activated complexes **4f** and **4g** have been previously reported by us.[8] Compounds **1e**−**g**, **2**, and **3** were prepared using the formic acid-catalyzed condensation of the appropriate aniline with the corresponding diketone in methanol. These conditions were not optimal for the preparation of α-diimines containing electron-withdrawing groups. Thus **1a**−**d** were prepared by the reaction of diketone with amine in the presence of catalytic amounts of H_2SO_4, in toluene with removal of water by azeotropic distillation. We have fully characterized the previously unknown ligands by ^1H, ^{13}C, and, where appropriate, ^{19}F NMR spectroscopy as well as elemental analysis. Compounds **1a**−**d** exhibit a complex fluctional behavior in solution which involves interconversion between (*E*, *E*) and (*E*, *Z*) forms as well as net rotation about the carbon−nitrogen aryl bond to interconvert syn and anti isomers. A complete analysis of this fluctional behavior is beyond the scope of this paper, but a similar behavior has been reported.[38] Interestingly, **2** was isolated and characterized spectroscopically, not as the α-diimine but rather as the imine/enamine tautomer. This tautomerization has also been observed for a similar compound which was reported by van Asselt and co-workers,[38] as well as a *β*-diimine ligand reported by Feldman et al.[16]

As previously reported, the nickel(II) dibromide complexes were readily obtained from reaction of the α-diimine with (DME)$NiBr_2$.[39] Characterization of these complexes was difficult because of their poor solubility in organic solvents, and the fact that they are paramagnetic, and thus high-resolution NMR spectroscopic analysis is not possible. Fortunately, crystals of **4c** and **4d** which were suitable for X-ray diffraction analysis were obtained by slow diffusion of pentane into a dichloromethane solution of the Ni(II) complexes.

The crystal structure of **4c** (Figure 1) with a 2-pentafluorophenyl substituent crystallized with two molecules of water coordinated to nickel, making this a six-coordinate octahedral complex. As in related structures,[17,38] the aryl rings of the α-diimine lie nearly perpendicular to the plane formed by the metal and coordinated nitrogen atoms. Of particular note is the C_2 symmetry of the complex about the nickel atom, with the pentafluorophenyl rings in a anti conformation above and below the coordination plane. Similarly, complex **4d** (Figure 2) crystallizes with the pentafluorophenyl rings in the anti conformation, but in this case, no water was coordinated to the tetrahedral nickel center. However, in both cases, this does not preclude the alternative conformation in which the pentafluorophenyl groups are in a syn conformation. In both structures, the pentafluorophenyl rings are oriented with the face of each ring directed approximately over the axial sites of the nickel atom.

B. Polymerization Experiments at 35 °C. While well-defined catalysts of the type [(α-diimine)$Ni(CH_3)$-(solv)]$^+$ BAr'_4 (Ar′ = 3,5-$(CF_3)_2C_5H_3$; solv = OEt_2) can be prepared, these salts are exceedingly sensitive to moisture, air, and heat.[8,32] A much more convenient method for generation of catalysts involves in situ activation of the nickel(II) dibromide complexes with methylaluminoxane (MAO) or its derivatives.[8,9] In this study, we have consistently employed modified methylaluminoxane (MMAO; see Experimental Section for details) as the activator. To make meaningful comparisons of the effect of catalyst structure on catalyst activity and polymer structure and properties, all data were collected under similar conditions. A temperature

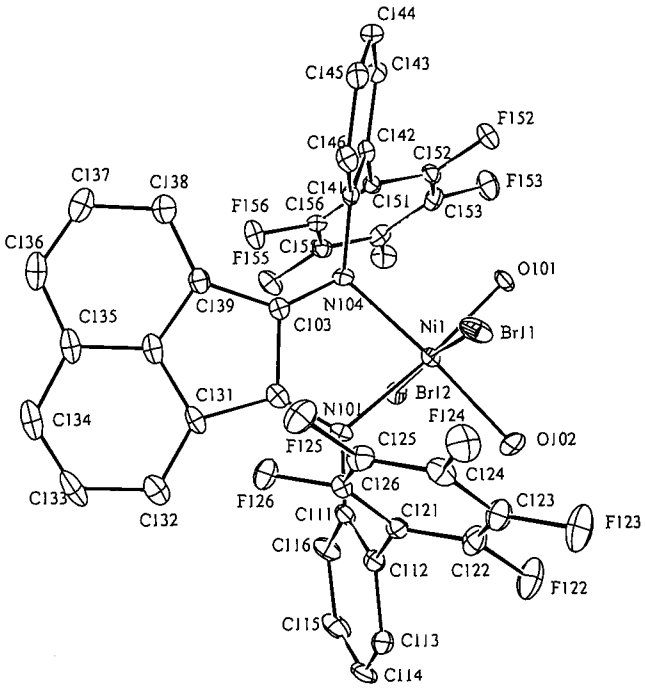

Figure 1. Molecular structure of **4c**. Selected bond lengths (Å) and angles (deg): Ni(1)−Br(11) 2.493(1), Ni(1)−Br(12) 2.612(8), Ni(1)−O(101) 2.063(3), Ni(1)−O(102) 2.100(3), Ni(1)−N(101) 2.109(4), Ni(101)−C(102) 1.283(6), C(102)−C(103) 1.515(7), C(103)−N(104) 1.280(6), N(1)−N(104) 2.093(4); Br-(11)−Ni(1)−Br(12) 174.41(3), N(101)−Ni(1)−N(104) 80.3(1), Ni(1)−Ni(101)−C(102) 111.0(3), Ni(101)−C(102)−C(103) 134.9-(5), C(102)−C(103)−N(104) 117.6(4), C(103)−N(104)−Ni(1) 112.1(3).

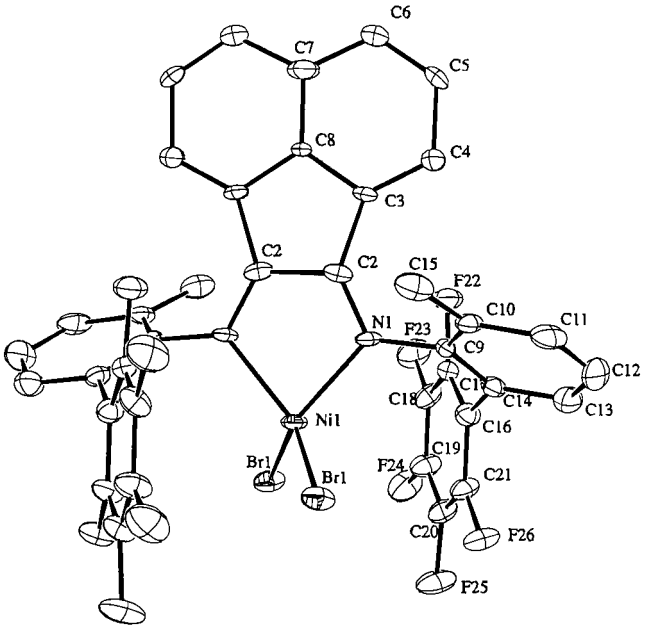

Figure 2. Molecular structure of **4d** (molecule 1). Selected bond lengths (Å) and angles (deg). Molecule 1: Ni(1)−Br(1) 2.323(1), Ni(1)−N(1) 2.035(7), Ni(1)−C(2) 1.296(11), C(2)−C(2)a 1.48(2); Br(1)−Ni(1)−Br(1)a 117.43(7), N(1)−N(1)−N(1)a 82.4(3), Ni(1)−Ni(1)−C(1) 111.6(6), Ni(1)−C(2)−C(2)a 117.2-(7). Molecule 2: Ni(2)−Br(2) 2.288(1), Ni(2)−N(31) 2.013(6), N(31)−C(32) 1.279(11), C(32)−C(32)b 1.47(2); Br(2)−Ni(2)−Br(2)b 123.44(8), N(31)−Ni(2)−N(31)b 83.0(3), N(2)−N(31)−C(32) 110.6(5), N(31)−C(32)−C(32)b 117.7(7).

Table 1. Polymerization Data for Experiments at 35 °C, 1 atm of C_2H_4

entry	catalyst	mol of catal ($\times 10^6$)	temp (°C)	reacn time (min)	TOF ($\times 10^{-3}$/h)	M_n[a]	PDI	branches per 1000 carbons	thermal transitions (°C) T_g	thermal transitions (°C) T_m
1	**4a**	2.0	30	30	150	4100[b]		31[c]		92, 107
2	**4b**	2.0	35	30	45	240 000	2.5	75	−40	56
3	**4c**	2.8	35	20	4	1020[b]		29[c]		
4	**4d**	3.7	35	20	5	41 400	4.4	34		107
5	**4e**	10	35	30	8	920[b]		3[c]		
6	**4f**	2.0	35	30	24	14 300	1.8	67	−44	29, 60
7	**4g**	1.6	35	30	56	125 000	1.8	106		−17
8	**5**	1.8	35	30	30	268 000	1.5	108		−8
9	**6**	1.8	35	30	15	171 000	1.6	101	−52	−2

[a] Molecular weights of the polymers were determined by GPC (using a universal calibration) in trichlorobenzene at 135 °C. [b] Molecular weights of low molecular weight samples were determined by end group analysis using ^{1}H NMR spectroscopy. [c] Branching numbers for low molecular weight samples (M_n < 5000) were corrected for end groups.

Table 2. Polymerization Experiments at 35 °C, 200 psig of C_2H_4

entry	catalyst	mol of catal ($\times 10^6$)	temp (°C)	pressure (psig)	reacn time (min)	TOF ($\times 10^{-3}$/h)	M_n[a]	PDI	branches per 1000 carbons	thermal transitions (°C)
1	**4a**	1.1	35	200	20	1100	3800[b]		5[c]	125 (T_m)
2	**4b**	2.0	35	200	20	500	400 000	3.3	27	127 (T_m)
3	**4c**	1.7	35	200	20	650	970[b]		5[c]	
4	**4d**	0.5	35	200	20	1100	73 700	2.6	4	134 (T_m)
5	**4e**	5.0	35	200	20	230	1300[b]		2[c]	
6	**4f**	1.5	35	200	10	1600	59 200	2.5	13	128 (T_m)
7	**4g**	0.83	35	200	10	2400	337 000	1.8	24	110 (T_m)
8	**5**	0.89	35	200	10	1600	844 000	1.7	39	100 (T_m)
9	**6**	0.95	35	200	10	900	766 000	1.7	28	96 (T_m)

[a] Molecular weights of the polymers were determined by GPC (using a universal calibration) in trichlorobenzene at 135 °C. [b] Molecular weights of low molecular weight samples were determined by end group analysis using ^{1}H NMR spectroscopy. [c] Branching numbers for low molecular weight samples (M_n < 5000) were corrected for end groups.

of 35 °C was chosen for the initial polymerization experiments because of the ease in maintaining constant temperature in both the ambient pressure runs and, more importantly, the high pressure runs. The reactions at high ethylene pressures are observed to exotherm rapidly as the reactor is pressurized and throughout the polymerization run. Thus, a reaction starting at room temperature (25 °C) can rapidly warm to >60 °C throughout a 10−20 min experiment without efficient cooling. The most reproducible reaction temperatures for runs conducted at 35 °C were obtained when the reactor was initially stabilized at 27 °C; upon addition of the activator (MMAO) and the catalyst, and subsequent pressurization with ethylene, the temperature in the reactor then rapidly rose to 35 °C within ca. 30 s, where it could be maintained by cooling with an ice-cooled water circulator for the rest of the run (10 or 20 min).

1. Effects of Varying Ligand Structure on Catalyst Activity and Polymer Properties. The results for ethylene polymerization experiments conducted at 1 atm and 35 °C are shown in Table 1, and polymerizations run at 35 °C and 200 psig (ca. 15 atm) are summarized in Table 2. Reactions run at 1 atm of ethylene pressure suffer from monomer mass transport limitations at this low ethylene concentration,[40] and therefore accurate comparisons of catalyst turnover frequencies (TOF)[41] are difficult under these conditions. Monomer mass transport is not a factor when the ethylene pressure is raised to 200 psig, and thus, a more accurate determination of the high turnover frequencies attainable by these catalysts is possible. In addition, comparison of trends in turnover frequencies for these catalysts can be made at this pressure.

A striking feature observed in the data is that the catalysts with only one *ortho* substituent on the aryl rings, R [R = CF_3 (**4a**), C_6F_5 (**4c**), CH_3 (**4e**); Table 1, entries 1, 3, and 5], do not yield a high molecular weight polymer but instead produce oligomers for which olefinic end groups could be detected by ^{1}H NMR spectroscopy (% α-olefin: **4a**, 55%; **4c**, 35% **4e**, 37%). Integration of the olefinic ^{1}H resonances with respect to the methylene resonances gave degrees of polymerization (DP) less than 150.

When a methyl substituent is introduced into the remaining *ortho* position of these catalysts the polymer molecular weight increases dramatically (see Table 1). For example, if **4a** (2-CF_3) is compared with **4b** (2-CF_3, 6-CH_3), the M_n increases from 4100 to 240 000. Similar trends are noted for **4c** (2-C_6F_5) vs **4d** (2-C_6F_5, 6-CH_3) (M_n = 1020 and 41 400, respectively) and **4e** (2-CH_3) vs **4f** (2,6-CH_3) (M_n = 920 vs 14 300). Polymerizations carried out at 200 psig and 35 °C (Table 2) exhibit similar trends. For example, **4a** yields polyethylene with M_n = 3800 while **4b** yields polyethylene with M_n = 400 000. Similarly, molecular weights of polyethylenes formed by catalysts **4d** and **4f** under these conditions were significantly higher than polyethylenes prepared with **4c** and **4e**, respectively. These observations are all in accord with our previous observation that increased steric bulk in the axial sites will lead to a decrease in the rate of chain transfer relative to the rate of propagation.

It is significant to note that the molecular weight distributions of polyethylene formed by **4b** and **4d** at 1 atm are 2.5 and 4.4, respectively, which are substantially broader than those for the polyethylenes produced by the other catalysts. A possible explanation for this broadening is that two isomers of complexes **4b** and **4d** are present, a C_2 symmetric form, and a C_s symmetric form. Species of both symmetries may be formed when

the nickel complexes are synthesized;[42] thus, the broadening of the molecular weight distribution may be attributable to the presence of more than one type of catalyst in solution. However, it was not possible to resolve a bimodal feature by GPC, and we have no additional evidence for a two-site catalyst system.

The measured turnover frequencies (TOF's) of these catalysts are affected by several variables and are often difficult to interpret.[43] For example, for highly active catalysts, mass transfer limitations may apply, and at 1 atm of ethylene pressure, it is clear that these effects do limit observed turnover frequencies of the active catalysts in Table 1. Catalyst instability can reduce calculated TOF's in runs over extended time periods or at high temperatures (see below) relative to conditions where no catalyst decay occurs. In cases where insoluble polymer is formed, TOF's often fall when catalysts become heterogeneous due to precipitation. In addition, of course, TOF's are affected by electronic[12] and steric effects of substituents. Under conditions reported in Table 2 (low catalyst loading, 200 psig, 35 °C, short reaction time), previous experiments,[44] together with those discussed below, suggest that mass transfer limitations do not apply, the catalyst resting state is the nickel alkyl ethylene complex, and catalysts are stable over these time periods at 35 °C. Thus, the observed differences in TOF's in Table 2 can be largely attributed to substituent effects.

The basic trend observed, consistent with previous observations, is that increases in the bulk of the *ortho* substituents result in increased TOF's. For example, the TOF of **4g** (2,6-di-^{i}Pr) is 2.4×10^6 h^{-1} compared to the less bulky **4f** (2,6-di-Me) of 1.6×10^6 h^{-1}. Consistent with this trend, the TOF of the monomethyl substituted catalyst, **4e**, drops to 2.3×10^5 h^{-1}. Similarly, the TOF of **4d** (2-C_6F_5, 6-CH_3) of 1.1×10^6 h^{-1} is about twice that of the TOF of the less bulky **4c** (2-C_6F_5) of 6.5×10^5 h^{-1}. The one catalyst pair which exhibits the opposite trend is **4a** (2-CF_3) with a measured TOF of 1.1×10^6 h^{-1} vs **4b** (2-CF_3, 2-CH_3) with a TOF of 5.0×10^5 h^{-1}. A possible explanation here may involve the rapid precipitation of the high molecular weight polymer formed by **4b** and thus, even under these conditions, reduction of the measured TOF due to precipitation.

The mono-CF_3 substituted catalyst **4a** is considerably more active than the mono-CH_3 system **4e** (1.8×10^6 h^{-1} vs 2.3×10^5 h^{-1} TOF). While part of the explanation may be steric, the fairly similar sizes of $-CF_3$ vs $-CH_3$ groups suggests also that the electron-withdrawing nature of the $-CF_3$ group, which results in a more electrophilic nickel center, may increase the TOF. This result is consistent with substituent effects noted in ethylene oligomerization reactions.[12]

Since the catalyst resting state under these conditions is the alkyl olefin complex, the TOF's (assuming no complications as enumerated above) will simply be the rate of migratory insertion. The fact that bulkier substituents accelerate this rate can be ascribed to more relief of strain in going from the more crowded ground-state alkyl olefin complex to the less crowded transition state.[35]

A strong correlation exists between the magnitude of steric bulk exerted by the *ortho* substituents and the degree of branching observed in the resulting polymers. The branching numbers for polyethylene can be determined by ^{1}H NMR spectroscopy using the ratio of the number of methyl groups to the overall number of carbons (e.g., methyl + methylene + methine),[45] and are reported as branches per thousand carbons.

In general, the branching numbers were observed to increase with more steric bulk (Table 1). For example, in experiments run under 1 atm of ethylene pressure, the branching number determined for polyethylene prepared using catalyst **4f** is 67, whereas 106 branches were observed when bulkier **4g** was employed. In addition, a comparison of the branching numbers for the series of catalysts with single substituents in the 2-position of the aryl rings (i.e., **4a**, **4c**, and **4e**) and catalysts containing substituents in the 2- and 6-positions (i.e., **4b**, **4d**, **4f**, and **4g**), shows that the branching is consistently higher for the latter catalysts. For example, catalyst **4a** (2-CF_3) yields polyethylene with 31 branches per thousand carbons whereas the bulkier catalyst **4b** (2-CF_3, 6-CH_3) affords polyethylene with 75 branches per thousand carbons.

These observations suggest that trapping of the intermediate alkyl cation (e.g., **B**, Scheme 2) by ethylene is slowed by bulky substituents more than the rate of chain running. Thus, more chain running and branching can occur in the catalysts that bear bulky substituents relative to those which possess less bulky substituents. The same trend is also noted in the 200 psig polymerizations (Table 2); however, at this increased pressure branching is reduced for all catalysts since the rate of trapping and insertion is now faster for all catalysts. This feature will be further illustrated and discussed below.

In our earlier communication, we reported that changes to the α-diimine backbone can have a remarkable effect on polymer microstructure and catalyst activity.[8] We have investigated this backbone effect further using complexes **4g**, **5**, and **6**, all of which contain the same bulky 2,6-di(isopropyl)phenyl groups as imine substituents. Complex **4g** contains a planar acenaphthyl backbone, whereas the other two catalysts, **5** and **6**, contain saturated alkyl groups as substituents on the backbone carbons. All three catalysts are very active polymerization catalysts (entries 7−9, Tables 1 and 2) with turnover frequencies on the order of 10^5/h at 1 atm and 10^6/h at 200 psig. Catalyst **4g** exhibits a slightly higher turnover frequency (2.4×10^6/h at 200 psig) than **5** and **6** (1.6×10^6 and 9.0×10^5/h, respectively).

Although the turnover frequencies are higher for **4g**, the molecular weights of polyethylene produced with catalyst **4g** are less than the molecular weights for polyethylene produced with catalysts **5** and **6**. For example, for polymerization experiments conducted at 200 psig, the molecular weight (M_n) of polymer generated from catalyst **4g** was 337 000 whereas from catalysts **5** and **6** the molecular weights were 844 000 and 766 000, respectively. A significant effect of the alkyl-substituted backbone is that the molecular weight distributions of the polyethylene are less than those produced by the planar acenaphthyl systems. This effect on molecular weight distributions can be seen clearly in Figure 3, which shows the GPC chromatograms for polyethylene produced with catalysts **4g**, **5**, and **6** at 1 atm and 35 °C. The polydispersity of polyethylene formed with catalysts **5** (Figure 3b) and **6** (Figure 3c) are 1.5 and 1.6, respectively (1 atm of ethylene; 35 °C), compared with 1.8 for the polymer produced by **4g** (Figure 3a) under identical conditions. When the ethylene pressure is raised to 200 psig, polydispersities

Table 3. Effect of Varying C_2H_4 Pressure on Polymer Properties and Catalyst Activities

entry	catalyst	mol of catal ($\times 10^6$)	temp (°C)	pressure (psig)	reacn time (min)	TOF ($\times 10^{-3}$/h)	M_n[a]	PDI	branches per 1000 carbons	thermal transitions (°C)
1	**4a**	1.1	35	200	20	1100	3800[b]		5[c]	125 (T_m)
2	**4a**	0.8	35	400	20	1300	4100[b]		4[c]	131 (T_m)
3	**4a**	0.8	35	600	20	2800	4000[b]		2[c]	119 (T_m)
4	**4b**	2.0	35	200	20	500	400 000	3.3	27	127 (T_m)
5	**4b**	2.0	35	400	20	560	533 000	2.8	5	130 (T_m)
6	**4b**	2.0	35	600	20	1000	314 000	3.7	7	131 (T_m)
7	**4c**	1.7	35	200	20	650	970[b]		5[c]	
8	**4c**	1.8	35	400	20	970	715[b]		3[c]	
9	**4c**	1.9	35	600	20	1600	776[b]		2[c]	
10	**4d**	0.5	35	200	20	1100	73 700	2.6	4	134 (T_m)
11	**4d**	0.5	35	400	20	1300	94 000	2.2	1	137 (T_m)
12	**4d**	0.5	35	600	20	1200	90 300	2.3	1	138 (T_m)
13	**4f**	1.5	35	200	10	1600	59 200	2.5	13	128 (T_m)
14	**4f**	1.5	35	400	10	1900	64 400	2.2	12	126 (T_m)
15	**4f**	1.5	35	600	10	2500	59 300	2.6	5	132 (T_m)
16	**4g**	0.83	35	200	10	2400	337 000	1.8	24	110 (T_m)
17	**4g**	0.83	35	400	10	3700	226 000	2.4	19	106 (T_m)
18	**4g**	0.81	35	600	10	3000	318 000	2.4	17	119 (T_m)
19	**5**	0.89	35	200	10	1600	844 000	1.7	39	100 (T_m)
20	**5**	0.85	35	400	10	2800	1 010 000	1.7	11	108 (T_m)
21	**5**	0.91	35	600	10	2600	799 000	1.9	11	114 (T_m)
22	**6**	0.95	35	200	10	900	766 000	1.7	28	96 (T_m)
23	**6**	0.86	35	400	10	2000	1 030 000	1.6	16	105 (T_m)
24	**6**	0.86	35	600	10	2300	1 000 000	1.6	15	105 (T_m)

[a] Molecular weights of the polymers were determined by GPC (using a universal calibration) in trichlorobenzene at 135 °C. [b] Molecular weights of low molecular weight samples were determined by end group analysis using ^{1}H NMR spectroscopy. [c] Branching numbers for low molecular weight samples (M_n<5000) were corrected for end groups.

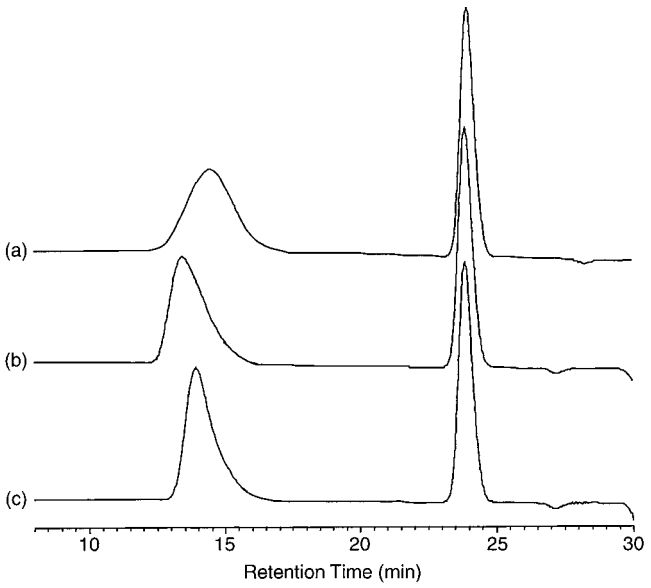

Figure 3. GPC chromatograms of polyethylene produced at 35 °C and 1 atm (ethylene) using catalyst: (a) **4g**; (b) **5**; (c) **6**.

increase slightly, but still remain below 2.0. The fact that molecular weight distributions remain below 2 under these conditions implies that the M_n values are not yet limited by chain transfer and longer reaction times would produce higher molecular weight materials.

2. Effects of Changes in Ethylene Pressure on Polymer Properties. A series of polymerization experiments in which the ethylene pressure was varied, but the temperature held at 35 °C, is summarized in Table 3. These data can be compared to that in Table 1 for polymerizations carried out at 1 atm of ethylene pressure. The most significant effect noted in these studies is a trend toward more linear, less branched polymers as the ethylene pressure is increased. For example, catalyst **4f** (2,6-di-CH_3) exhibits 67 branches per thousand carbons at 1 atm which drops to 13 branches per thousand carbons at 200 psig and to ca. 5 branches per thousand carbons at 600 psig of ethylene. Melting points (T_m's) determined using DSC range from 60 °C (a broad transition) to 132 °C (sharp transition) for these branching numbers. Similarly, catalyst **5** yields polyethylene containing 108 branches per thousand carbons at 1 atm of ethylene, 39 branches per thousand carbons at 200 psig, and 11 branches per thousand carbons at pressures of 400 and 600 psig. T_m values for these likewise increase with decreasing branching. Catalyst **4b** (2-CF_3, 6-CH_3) yields polyethylene with 75 branches per thousand carbons at 1 atm of ethylene, 27 branches per thousand carbons at 200 psig, and 5−7 branches per thousand carbons at 400 and 600 psig. An unusual feature of the polyethylene made at 200 psig is that despite it having 27 branches per thousand carbons, the T_m is remarkably high (127 °C) in comparison to the other polyethylene samples with similar branching numbers (see entry 4).

The trend of decreased branching with increasing ethylene pressure in these cases reinforces our earlier observations. In essence, chain running occurs in the cationic alkyl complex (**B**; Scheme 2) and the lifetime of this complex (and thus the extent of chain running) is decreased as ethylene concentration increases. The rate of insertion (chain growth) will either be *independent* of ethylene pressure if the resting state is predominantly the alkylolefin complex (**A**; Scheme 2) or *increase* with ethylene pressure if a significant fraction of the catalyst rests as the cationic alkyl complex (e.g., if the polymerization is mass transfer limited).

There is little variation of molecular weight with ethylene pressure for individual catalysts. The small variations observed are likely due to variations in experimental conditions (e.g., polymer precipitation and variable extent of catalyst decay) since no clear trend is observed as pressure is varied. The trends apparent in comparing different catalysts are consistent with the

Table 4. Polymerization Data for Experiments at 1 atm of C_2H_4 and 35, 60, and 85 °C

entry	catalyst	mol of catal ($\times 10^6$)	temp (°C)	reaction time (min)	TON ($\times 10^{-3}$)	M_n[a]	PDI	branches per 1000 carbons	thermal transitions (°C) T_g	thermal transitions (°C) T_m
1	**4b**	2.0	35	30	23	240 000	2.5	75	−40	56
2	**4b**	2.0	60	30	3.8	56 000	2.8	90	−44	
3	**4b**	2.0	85	30	dec	N/A				
4	**4g**	1.6	35	30	28	125 000	1.8	106		−17
5	**4g**	1.6	60	30	17	48 600	2.7	122	−65	−43
6	**4g**	1.6	85	30	5	27 000	2.7	124	−67	
7	**5**	1.8	35	30	15	268 000	1.5	108		−8
8	**5**	2.1	60	30	10	139 000	2.0	115	−60	−30
9	**5**	1.6	85	30	1.8	56 000	1.9	136	−60	
10	**6**	1.8	35	30	7.5	171 000	1.6	101	−52	−2
11	**6**	2.1	60	30	5.5	129 000	1.6	100	−40	−17
12	**6**	1.7	85	30	0.6	42 000	2.2	112	−53	−17

[a] Molecular weights of the polymers were determined by GPC (using a universal calibration) in trichlorobenzene at 135 °C.

Table 5. Polymerization Data for Experiments at 200 psig of C_2H_4 and 35, 60, and 85 °C

entry	catalyst	mol of catal ($\times 10^6$)	temp (°C)	pressure (psig)	reacn time (min)	TON ($\times 10^{-3}$)	M_n[a]	PDI	branches per 1000 carbons	thermal transitions (°C) T_g	thermal transitions (°C) T_m
1	**4b**	2.0	35	200	20	170	400 000	3.3	27		127
2	**4b**	2.0	60	200	20	140	237 000	3.3	46		102
3	**4b**	2.0	85	200	20	30	68 000	4.4	52	−37	81
4	**4d**	0.5	35	400	20	430	94 000	2.2	1		137
5	**4d**	0.5	60	400	20	950	53 900	1.9	12		130
6	**4d**	0.5	85	400	20	520	29 400	2.1	19		121
7	**4f**	1.5	35	200	10	270	59 200	2.5	13		128
8	**4f**	1.5	60	200	10	150	22 800	2.3	25		114
9	**4f**	2.0	85	200	10	25	12 900	2.9	44		90, 114
10	**4g**	0.83	35	200	10	400	337 000	1.8	24		110
11	**4g**	0.82	60	200	10	230	155 000	1.8	58	−42	68
12	**4g**	0.82	85	200	10	70	62 700	1.9	83	−45	24
13	**5**	0.89	35	200	10	270	844 000	1.7	39		100
14	**5**	0.89	60	200	10	130	395 000	1.7	60	−42	57
15	**5**	0.92	85	200	10	50	211 000	1.8	93	−50	20
16	**6**	0.95	35	200	10	150	766 000	1.7	46		96
17	**6**	0.83	60	200	10	100	331 000	1.9	73	−44	54
18	**6**	0.92	85	200	10	10	196 000	1.8	85	−49	23

[a] Molecular weights of the polymers were determined by GPC (using a universal calibration) in trichlorobenzene at 135 °C.

discussions above for the 1 atm results; that is, increasing the steric bulk of *ortho* substituents results in increasing polymer molecular weight. For catalyst **6**, M_n values reach 1×10^6 and are not yet limited by chain transfer processes since M_w/M_n values are still below 2.

C. Polymerization Experiments at Higher Temperatures. The experiments described above have all been carried out at 35 °C. In this section, we report polymerizations at higher temperatures and the impact of increasing temperature on catalyst activities and lifetimes as well as on polymer branching and molecular weights.

In general, at 60 °C and above, catalyst lifetimes are sufficiently short that they have a significant impact on the total turnovers (TON) which can be achieved over 10−30 min time periods. While a decrease in ethylene solubility at increased temperatures may play a role, it is clear that the major effect on total turnover number is catalyst decay. Table 4 reports polymerizations carried out at 1 atm and temperatures of 35, 60, and 85 °C. For catalyst **4b** (2-CF_3, 6-CH_3) the TON calculated for a 30 min run decreases from 23 000 at 35 °C to 3800 at 60 °C. At 85 °C, catalyst decay is sufficiently rapid that no polymer is isolated. Similar behavior is observed for **4g**, **5**, and **6** except that at 85 °C some activity is observed for these catalysts.

Table 5 reports polymerizations at 200 psig at 35, 60, and 85 °C. At 200 psig of ethylene pressure, considerably higher TON's are achieved relative to 1 atm runs. In general, TON's at 60 °C decrease by a factor of 2 or less relative to those observed at 35 °C, but at 85 °C TON's drop off quite significantly. For example, for **4b** the TON decreases from 170 000 (20 min run) at 35 °C to 140 000 at 60 °C, but then drops to 30 000 at 85 °C. For **4d** (2-C_6F_5, 6-CH_3) the TON increases to 950 000 at 60 °C from 430 000 at 35 °C and then drops to 520 000 at 85 °C.

The productivity of catalyst **5** was examined over 10−20 min reaction times at 60 and 85 °C at 200 psig (see Table 6). At 60 °C there is a significant increase in TON from the 10 min run (130 000) to the 20 min run (200 000) indicating that a significant fraction of the catalyst is still active after 10 min. However, at 85 °C the minor increase in TON at 20 min (64 000) relative to 10 min (53 000) reaction time indicates that most of the catalyst has deactivated after 10 min at 85 °C.

The mode of catalyst decay is unknown. One possibility for decay is a C−H activation of an *ortho* alkyl substituent.[46] Thus, our motivation for preparing catalysts containing *ortho* $-C_6F_5$ and $-CF_3$ substituents was the possibility that these catalysts would exhibit much higher stabilities than those possessing *ortho*− alkyl substituents. We have noted that TON's for polymerizations using catalyst **4d** (2-C_6F_5, 6-CH_3) remain high for

Table 6. Catalyst Lifetime Data for 5/MMAO at 200 psig of C_2H_4 and 60 and 85 °C

entry	mol of catal ($\times 10^6$)	temp (°C)	pressure (psig)	reacn time (min)	TON ($\times 10^{-3}$)	M_n[a]	PDI	branches per 1000 carbons
1	0.89	60	200	10	129	395 000	1.7	60
2	0.84	60	200	20	201	407 000	1.8	71
3	0.92	85	200	10	53	211 000	1.8	93
4	0.93	85	200	20	64	205 000	1.8	93

[a] Molecular weights of the polymers were determined by GPC (using a universal calibration) in trichlorobenzene at 135 °C.

Table 7. Ethylene Polymerization Activity vs Time for 4c/Mmao[a]

entry	mol of catal ($\times 10^6$)	reacn time (min)	temp (°C)	ethylene pressure (atm)	TON[b] ($\times 10^{-4}$)	M_n[c]	% α-olefin[c]	branches per 1000 carbons[c]
1	1.7	20	35	15	22	970	90	5
2	1.1	60	35	15	64	770	87	7
3	1.1	120	35	15	130	960	91	8
4	1.1	180	35	15	198	970	90	5
5	0.8	240	35	15	244	960	86	6
6	2.4	30	0	1	3.2	1020	77	5
7	2.5	60	0	1	6.1	1000	78	7
8	1.4	120	0	1	12.2	890	79	4
9	1.6	180	0	1	16.8	750	79	4
10	1.1	240	0	1	17.6	790	78	5

[a] Reaction conditions: 200 mL of toluene (entries 1−5) or 100 mL of toluene (entries 6−10), 1700 equiv of Al/equiv of Ni. [b] Turnover number. [c] Determined by ^{1}H NMR spectroscopy (corrected for end groups).

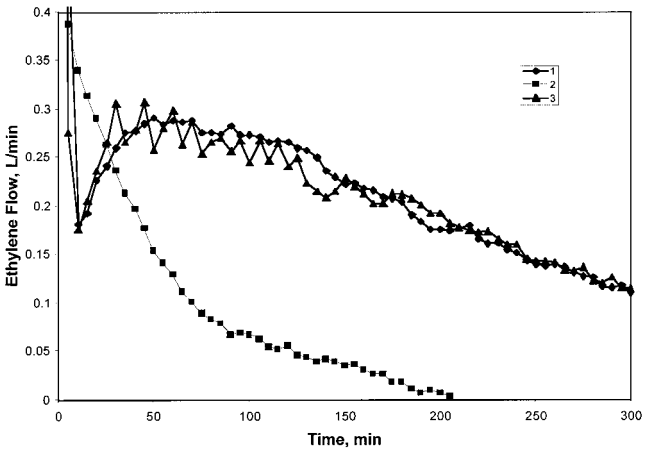

Figure 4. Ethylene flow profiles in polymerization reactions of **4c**/MMAO in toluene under 200 psig of ethylene pressure. Line 1: 400 mL of toluene 35 °C. Line 2: 400 mL of toluene, 60 °C. Line 3: 200 mL of toluene, 35 °C.

20 min runs at 60 and 85 °C and 200 psig of ethylene. However, we chose catalyst **4c** (2-C_6F_5) for stability studies since the low molecular weight polyethylene formed (ca. 900 M_n) does not form an insoluble polymer in the reactor, resulting in inactivity due to precipitation and inaccessibility of catalyst sites.[47] Results of a set of experiments monitoring productivity over time periods from 20 min to 4 h are summarized in Table 7. At 35 °C, 200 psig of ethylene, the productivity increases essentially linearly with time (entries 1−5). Thus, under these conditions, very little catalyst decomposition is occurring over this time period under these conditions. A similar set of experiments at 0 °C, 1 atm (entries 6−10) shows that activity does begin to decrease after 3−4 h, suggesting that catalyst stability is greater at higher ethylene pressures for this system.

Monomer flow measurements using **4c**/MMAO were conducted to gain additional data concerning catalyst activity. These data are summarized in Figure 4. At 35 °C and 200 psig of ethylene pressure, very slow catalyst deactivation was observed over a 5 h time period. The decay rate was independent of catalyst concentration. At 60 °C, the catalyst decay rate was considerably accelerated. Qualitatively, the stability of this catalyst is not significantly different from those bearing *ortho* alkyl substituents studied above. This latter experiment suggests that C−H bond activation is not a major route for deactivation of catalysts bearing *ortho* alkyl substituents.

The molecular weight of the polyethylene produced by each catalyst was found to decrease as the temperature was increased. For example, when catalyst **4b** (2-CF_3, 6-CH_3) is employed at 200 psig, the molecular weight drops from M_n = 400 000 when carried out at 35 °C to M_n = 237 000 at 60 °C and M_n = 68 000 at 85 °C. Similar effects are also observed with all the other catalysts, with a decrease in M_n of approximately 50% upon increasing the temperature by 25 °C. These results suggest that at higher temperatures there is an increase in the rate of chain transfer, although further complications with catalyst degradation may also affect molecular weights. The distribution of molecular weights is also observed to increase as the reaction temperature is increased.

The branching numbers are observed to increase dramatically with increasing temperature with a corresponding decrease in T_m values. For example, the branching numbers obtained for catalyst **5** increase from 39 per thousand carbons at 35 °C to 60 per thousand carbons at 60 °C to 93 per thousand carbons at 85 °C. This trend can be clearly observed by a comparison of the ^{1}H NMR spectra shown in Figure 5. The small doublet observed at δ = 0.83 ppm which is assigned to the methyl branches increases in intensity relative to the methylene resonances at δ = 1.24 ppm as the temperature is increased. Also, the methine resonances which are observed as broad resonances at δ = 1.1 ppm increase with increasing temperature. Furthermore, the fact that the methyl resonances are split into doublets indicates that the branches in these polyethylenes are mainly CH_3 branches, however the small shoulder visible at δ = 0.80 ppm suggests the presence of other longer branches.

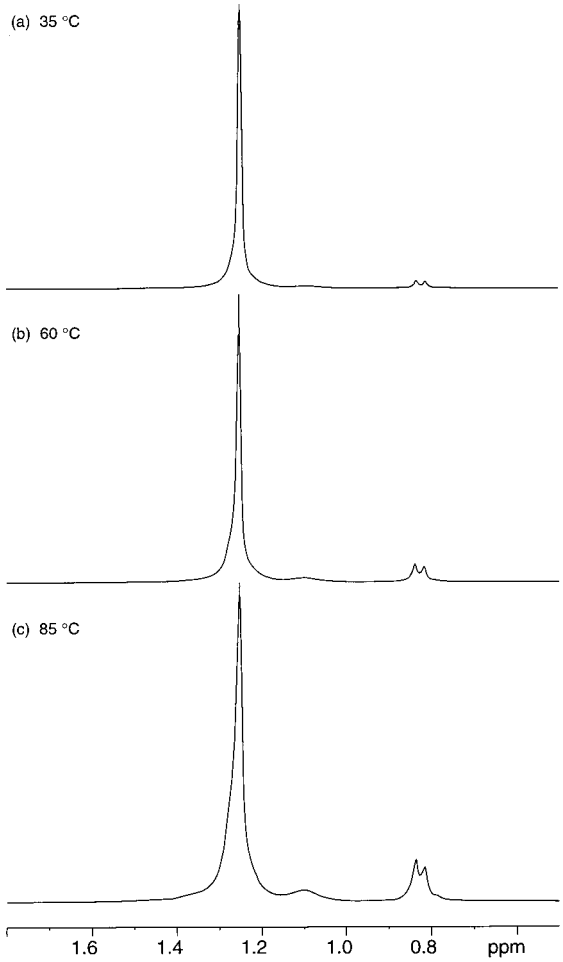

Figure 5. ^{1}H NMR spectra (300 MHz, C_6D_5Br, 120 °C of polyethylene prepared with catalyst **5**/MMAO at 200 psig of ethylene showing the effect of reaction temperature on branching.

E. Thermal Properties of Highly Branched Polyethylenes. The physical appearance of the unprocessed polyethylene samples isolated from the reactor varies dramatically as the nature of the catalyst structure changes. For example, polymers formed with bulky 2,6-di(isopropyl)phenyl-substituted catalysts (**4g**, **5** and **6**) at 1 atm and 35 °C are clear, colorless rubbery materials, whereas with catalyst **4b** a white rubbery material is formed. At 200 psig, the polymer formed with **4b** is a tough flexible white solid, and with **4g**, **5**, and **6**, the materials are rigid solids.

To gain insight into the thermal properties of these highly branched polyethylenes, we have characterized the polymers by differential scanning calorimetry (DSC).[48] The linear polymers (<5 branches per thousand carbons) were found to exhibit melt transitions (T_m's) between 125 and 135 °C, which is typical of high-density polyethylene (HDPE) which has a T_m of 135 °C.[49] For example, the linear polyethylene produced at high pressures with catalyst **4d** (see Table 3) has a branching number of only 1 per thousand carbons and a T_m of 137−138 °C. With other bulky catalysts (**4g**, **5**, and **6**), the branched materials produced at similar pressures exhibit melting points of ca. 100 °C.

A complex thermal behavior is observed for the highly branched polyethylenes prepared at 1 atm or 200 psig, which we attribute to the irregularity of the polymer structure. For example, the polyethylene produced at

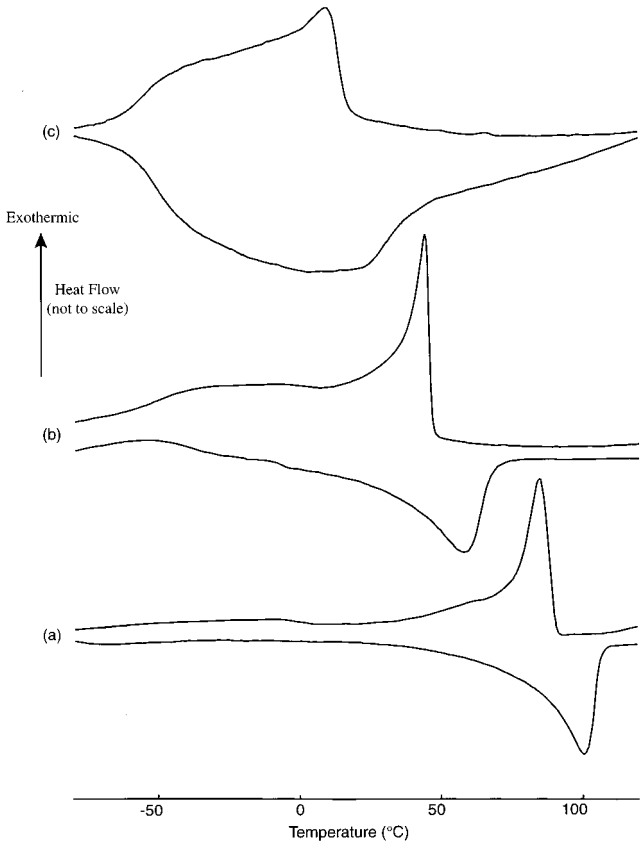

Figure 6. DSC thermograms of polyethylene prepared at 200 psig with catalyst **5**: (a) 35 °C; (b) 60°; (c) 85 °C.

35 °C with catalysts **5** and **6** (108 and 101 branches per thousand carbons, respectively) show melting transitions below room temperature (−8 and −2 °C, respectively), and each also exhibit a second-order transition. As the branching numbers increase (at higher temperatures), the second-order transition becomes more pronounced, and the melting points shift to lower temperature and occur over a much broader temperature range. For example, Figure 6 shows the DSC thermograms for polyethylene prepared using catalyst **5** at 200 psig at temperatures of 35, 60, and 85 °C. The polyethylenes produced at 35 °C (Figure 6a) and 60 °C (Figure 6b) exhibit broad melting transitions on the heating curves; however, they are much sharper upon crystallization on the cooling curve. In addition, the second-order transition at ca. −42 °C, which is barely visible on the heating curve, is clearly observed on the cooling curve. The second-order transition is observed upon repeated scanning of the sample between −100 and 140 °C. This transition is even more pronounced for the polymer obtained from catalyst **5** at 85 °C (Figure 6c).

It is worth noting that the thermal properties of low-density polyethylene have been studied extensively, and three second-order transitions have been observed. The α transition usually occurs between 30 and 120 °C, the β transition is typically detected between −30 and +10 °C, and the γ transition is seen in the range of −150 to −120.[50,51] The second order transitions observed in this study are likely β transitions, which are usually observed using dynamic mechanical techniques,[52] and have been attributed to the onset of motion at branch points.[49,51] The unique highly branched structures of the present polymers makes the second-order transitions detectable by DSC. We have also carried out a dynamic

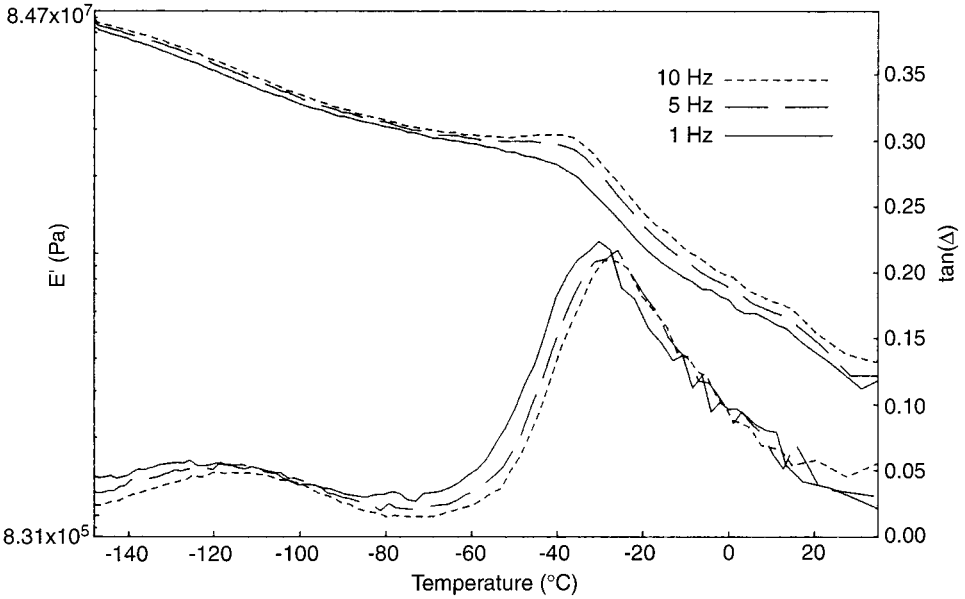

Figure 7. DMA of polyethylene produced using **4g**/MMAO (200 psig, 60 °C) with sampling frequencies of 10, 5, 2, 1, and 0.5 Hz (for clarity, only the 10, 5, and 1 Hz slices are shown). The top curve corresponds to E' while the bottom curve corresponds to tan(Δ).

mechanical analysis (DMA) experiment on a polyethylene fiber produced using catalyst **4g** (200 psig, 60 °C) (Table 5; entry 11), which is shown in Figure 7. The β transition is clearly observed at −30 °C (1 Hz) as the peak maximum in the tan(Δ) curve. This transition was observed at −42 °C by DSC. In addition, the γ transition was also detected at −126 °C. These results are consistent with those previously reported for low-density polyethylene.

Summary

Several conclusions can be drawn from these studies which reinforce our earlier observations concerning effects of ethylene pressure, temperature, and ligand variation on these ethylene polymerizations. All of the effects are completely consistent with our proposed mechanistic scheme for chain growth.

(1) As the bulk of the *ortho* aryl substituents on the α-diimine ligand increases, the molecular weights of the polyethylenes increase. With mono *ortho* substituted aryl α-diimine catalysts, M_n values as low as ca. 1000 are seen, while with the bulkiest *ortho* diisopropyl-substituted systems, M_n values reach 10^6.

(2) Increased steric bulk of the *ortho* substituents also increases the extent of branching in the polyethylenes as well as the turnover frequencies. The electron-withdrawing substituent, *o*-CF_3, appears to increase the TOF more than expected based simply on steric effects, and is consistent with earlier observed electronic effects.

(3) Catalysts bearing alkyl substituents on the backbone carbon atoms tend to give higher molecular weight polymers with more narrow molecular weight distributions than the catalysts bearing the planar aromatic acenaphthyl backbone. Catalyst activities are comparable.

(4) Increases in ethylene pressure lead to dramatic reductions in the extent of branching in the polymer presumably due to an increased rate of trapping and insertion relative to the rate of chain isomerization which is independent of C_2H_4.

(5) Increases in polymerization temperatures result in increased branching and decreased molecular weights. Catalysts are stable over hours at 35 °C, but lifetimes are reduced to minutes at temperatures above 60 °C. The catalyst decay mechanism is unknown, but results with fluorinated *ortho* substituents show decay is likely not due to C−H bond activation of *ortho* alkyl substituents.

The physical properties of the homopolyethylenes produced by these catalyst systems vary widely depending on the extent of branching and polymer molecular weight. It is clear from these studies that structural variations of the α-diimine ligand coupled with the conditions of polymerization (temperature and ethylene pressure) can be used to control branching and molecular weight in a predictable way. Thus, variably branched polyethylenes can be produced without the use of an α-olefin comonomer (as is required for early metal catalysts) with properties which not only span the range of HDPE to LLDPE to LDPE but also include amorphous, elastomeric homopolymers.

Experimental Section

General Methods. All manipulations of air- and/or water-sensitive compounds were performed using standard high-vacuum or Schlenk techniques. Argon was purified by passage through columns of BASF R3−11 catalyst (Chemalog) and 4-Å molecular sieves. Solid organometallic compounds were transferred in an argon-filled Vacuum Atmospheres drybox. ^1H, ^{13}C, and ^{19}F NMR spectra were recorded on Bruker Avance-500, -400, -300, or Varian Gemini 300 MHz spectrometers. Chemical shifts are reported relative to residual $CHCl_3$ (δ 7.24 for ^1H), $CDCl_3$ (δ 77.00 for ^{13}C), and CCl_3F (δ 0.00 for ^{19}F). ^1H NMR spectra of polyethylene were taken in C_6D_5Br at 120 °C. Ethylene flow measurements were made with an Omega FMA-869 mass flowmeter and recorded with an Omega RD-853-T paperless recorder. High-temperature gel permeation chromatography (GPC) was performed by DuPont (Wilmington, DE) in 1,2,4-trichlorobenzene at 135 °C using a Waters HPLC 150C equipped with Shodex columns. A calibration curve was established with polystyrene standards and universal calibration was applied using Mark−Houwink constants for polyethylene ($k = 4.34 \times 10^{-4}$; $\alpha = 0.724$). Differential scanning calorimetry was recorded on a Seiko Instruments DSC 220 calibrated with the melting transition of indium. Samples were heated to ca. 50 °C above their T_m and cooled rapidly to −120

Scheme 6. Labeling Schemes Used To Report NMR Data for 1a, 1c, 1d, and 2

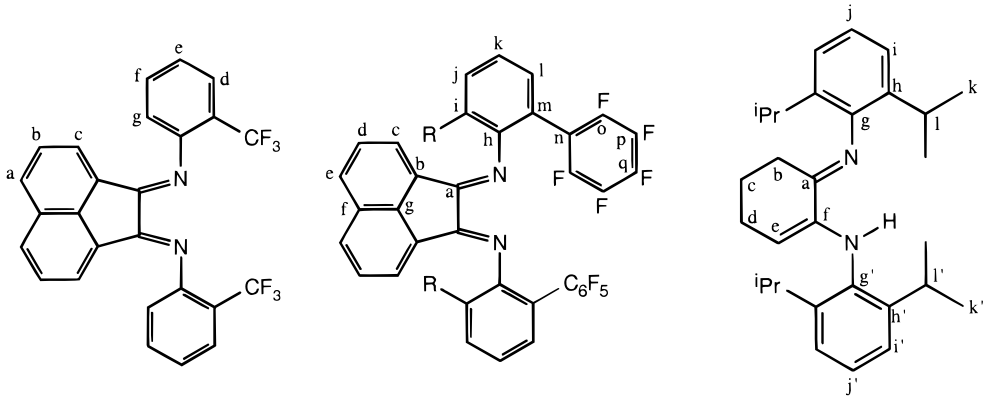

1a **1c (R = H)** **1d (R = CH_3)** **2**

°C and held for 20−30 min prior to scanning (scan rate: 10 °C/min). Dynamic mechanical analysis was carried out using a Seiko Instruments DMS210 with a scan rate of 2 °C/min between −150 and +50 °C, and frequencies of 10, 5, 2, 1, and 0.5 Hz. The polyethylene fibers were used as obtained from the reaction for the elemental analyses which were performed by Atlantic Microlab of Norcross, GA. Labeling diagrams for **1a**, **1c**, **1d**, and **2** are given in Scheme 6.

Materials. Toluene, diethyl ether, pentane, and methylene chloride were purified using procedures recently reported by Pangborn et al.[53] High pressure polymerizations were performed in a mechanically stirred 1000 mL Parr autoclave. Polymer-grade ethylene (99.5%) was purchased from National Specialty Gases and used without further purification. 7% Al (wt %) and 6.4% Al solutions of modified methylaluminoxane (MMAO) in heptane (d = 0.73 g/mL) containing 23−27% isobutyl groups were purchased from Akzo Nobel. Diimine ligands **1e**−**g**, **2**, and **3** as well as nickel(II) bromide complexes **4**−**6** were prepared according to modified literature procedures.[8,38,39,54] Acenaphthenequinone, aniline, 1,2-cyclohexanedione, iodopentafluorobenzene, 2,6-diisopropylaniline, 2,3-pentanedione, *o*-toluidine, 2-trifluoromethylaniline, and (DME)-$NiBr_2$, were purchased from Aldrich Chemical Co. C_6D_5Br was purchased from Cambridge Isotope Laboratories and stored over activated 4 Å molecular sieves. 2-(Pentafluorophenyl)-aniline[55] and 2-methyl-6-trifluoromethylaniline[56] were prepared according to literature procedures.

Synthesis of (ArN=C(An)-C(An)=NAr) (Ar = 2-$CF_3C_6H_4$) (1a). Acenaphthenequinone (2.73 g, 15.0 mmol) and *o*-trifluoromethylaniline (6.43 g, 40.0 mmol) were stirred in toluene (100 mL) and sulfuric acid (1 drop) was added. The solution was refluxed for 3 days using a Dean−Stark trap to collect H_2O eliminated. K_2CO_3 (5 g) was added at room temperature, the solution filtered and toluene removed in vacuo. The orange solid obtained was dissolved in CH_2Cl_2 (40 mL) and pentane (40 mL) was added. After 1 d at −30 °C, yellow-orange crystals formed which were isolated by filtration, and washed with pentane (2 × 10 mL), and dried in vacuo. Yield of **1a** = 5.70 g (81%). Two isomers are observed by NMR in a 3.8:1 ratio ($C_2D_2Cl_4$, 295 K); the major isomer has C_2 or C_s symmetry, while all resonances are unique for the minor isomer (C_1 symmetry). Many of the NMR resonances corresponding to the minor isomer are obscured by those from the major isomer and are therefore not reported. ^{1}H NMR (500 MHz, $C_2D_2Cl_4$, 295 K, major isomer): δ 7.86 (d, J = 8.0 Hz, 2 H, a), 7.73 (d, J = 8.0 Hz, 2 H, d), 7.57 (dd, J = 8.0, 7.5 Hz, 2 H, f), 7.34 (dd, J = 8.5, 7.5 Hz, 2 H, b), 7.31 (dd, J = 8.0, 7.5 Hz, 2 H, e), 7.04 (d, J = 8.0 Hz, 2 H, g), 6.57 (d, J = 7.0 Hz, 2 H, c). ^{13}C NMR (75 MHz, $CDCl_3$, 293 K, major isomer): δ 161.4, 149.9, 141.9, 132.9, 131.7 (q, $^1J_{CF}$ = 284 Hz, CF_3), 131.1, 129.3, 128.3, 127.8, 126.9 (q, $^3J_{CF}$ = 4.5 Hz), 124.0, 123.8, 118.8, 117.2 (q, $^2J_{CF}$ = 32 Hz). ^{19}F NMR (376 MHz, $C_2D_2Cl_4$, 293 K, major isomer): δ −61.6 (br s, CF_3). Anal. Calcd for $C_{26}H_{14}F_6N_2$: C, 66.67; H, 3.01; N, 5.98. Found: C, 66.55; H, 3.04; N, 5.92.

Synthesis of (ArN=C(An)−C(An)=NAr) (Ar = 2-Me-6-$CF_3C_6H_3$) (1b). Acenaphthenequinone (0.91 g, 5.0 mmol) and 2-methyl-6-trifluoromethylaniline (1.9 g, 11 mmol) were stirred in toluene (40 mL), and sulfuric acid (2 drops) was added. The solution was refluxed for 1 day using a Dean−Stark trap to collect H_2O eliminated. The ruby-red solution was filtered while still hot into a clean flask containing 5 g of K_2CO_3, and allowed to stand for 15 min. A second filtration to remove K_2CO_3, and solvent removal in vacuo, yielded an orange solid. The crude product was purified by column chromatography on 200−400 mesh, 60-Å silica gel using a gradient of 5% ethyl acetate/1% triethylamine/hexanes (initial) to 50% ethyl acetate/1% triethylamine/hexanes (final). The product eluted as the first major orange band and was isolated after solvent removal as a yellow solid. Yield of **1b** = 1.0 g (40%). The product NMR resonances are broad at room temperature; however, at 248 K the product exists as four distinct isomers (49:30:14:7 ratio). The two major isomers have C_2 or C_s symmetry, while the two minor isomers have C_1 symmetry. ^{1}H NMR (500 MHz, $C_2D_2Cl_4$, 248 K, most abundant isomer): δ 7.88 (d, J = 8.4 Hz, 2 H), 7.56 (d, J = 7.2 Hz, 2 H), 7.45 (d, J = 7.6 Hz, 2 H), 7.35 (pseudo t, 2 H), 7.20 (pseudo t, 2 H), 6.47 (d, J = 7.2 Hz, 2 H), 2.04 (s, 6 H, CH_3). ^{13}C{^{1}H} NMR (125 MHz, $C_2D_2Cl_4$, 243 K, most abundant isomer): δ 162.4, 148.3, 141.4, 135.1, 131.1, 130.1, 128.9, 128.8, 127.1, 126.4 (q, $^1J_{CF}$ = 293 Hz), 124.9, 124.2, 123.4, 117.7 (q, $^2J_{CF}$ = 31 Hz), 18.0. ^{19}F NMR (376 MHz, $C_2D_2Cl_4$, 243 K, most abundant isomer): δ −61.3 (s, CF_3). Anal. Calcd for $C_{26}H_{14}F_6N_2$: C, 67.74; H, 3.65; N, 5.64. Found C, 67.83; H, 3.68; N, 5.57.

Synthesis of (ArN=C(An)−C(An)=NAr) (Ar = 2-(C_6F_5)-C_6H_4) (1c). To a stirred solution of 2-(pentafluorophenyl)-aniline (1.0 g, 3.8 mmol) in 100 mL of toluene were added acenaphthenequinone (0.32 g, 1.7 mmol) and H_2SO_4 (0.01 mL, 0.1 mmol). After the reaction was refluxed for 48 h, the solvent was removed on a vacuum line, leaving the crude product as an orange residue. The crude orange residue was purified by column chromatography (15% ethyl acetate/hexanes, 60 mm silica gel) to yield the product as an orange solid. Yield: 0.4 g (30%). Two isomers are observed by NMR in a 3.5:1 ratio ($CDCl_3$, room temperature); the major isomer has a C_2 axis or C_s plane of symmetry, while all resonances are unique for the minor isomer (C_1 symmetry). Many of the NMR resonances corresponding to the minor isomer are obscured by those from the major isomer, and are therefore not reported. ^{1}H NMR (300 MHz, $CDCl_3$, 293 K, major isomer): δ 7.92 (d, $^3J_{HH}$ = 8.1 Hz, 2 H, e), 7.49 (dt, $^3J_{HH}$ = 7.6 Hz, $^4J_{HH}$ = 1.8 Hz, 2 H, j), 7.41 (t, $^3J_{HH}$ = 8.1 Hz, 2 H, d), 7.39 (t, $^3J_{HH}$ = 7.6 Hz, 2 H, k), 7.35 (broad d, $^3J_{HH}$ = 7.6 Hz, 2 H, l), 7.12 (d, $^3J_{HH}$ = 8.1 Hz, 2 H, c), 7.04 (d, $^3J_{HH}$ = 7.6 Hz, 2 H, i). ^{13}C{^{1}H} NMR (75 MHz, $CDCl_3$, 293 K, major isomer): δ 162.2 (a), 150.5 (h), 144.0 (broad d, $^1J_{CF}$ = 264 Hz, o), 141.9 (g), 140.7 (broad d, $^1J_{CF}$ = 226 Hz, q), 138.4 (broad d, $^1J_{CF}$ = 257 Hz, p), 132.1 (f), 131.3 (b), 130.6 (e), 129.5 (d), 128.0 (j), 127.6 (l), 124.9 (k), 124.0 (c), 119.0 (*C*-9), 116.9 (m), 113.5 (t, $^2J_{CF}$ = 23 Hz, n). ^{19}F NMR (282 MHz,

$CDCl_3$, 293 K, major isomer): δ −139.0 (broad, 4 F, F_{ortho}), −155.1 (t, $^3J_{FF}$ = 17.0 Hz, 2 F, F_{para}), −162.9 (broad, 4 F, F_{meta}). Anal. Calcd for $C_{36}H_{14}F_{10}N_2$: C, 65.07; H, 2.12; N, 4.22. Found: C, 65.12; H, 2.17; N, 4.22.

Synthesis of 2-Methyl-6-(pentafluorophenyl)aniline. Under a nitrogen atmosphere, a stirred solution of C_6F_5I (13.2 g, 44.9 mmol), *o*-toluidine (16.1 g, 149 mmol), and acetonitrile (150 mL) in a Pyrex flask was irradiated with a medium-pressure mercury lamp (450 W) for 3 days at 80 °C. The mixture was concentrated, and the residue was extracted with diethyl ether (100 mL). The ether solution was then washed with 5% aqueous $NaHCO_3$ and dried over $MgSO_4$, and the solvent was removed. Excess *o*-toluidine was removed via vacuum distillation. The oily residue was purified using column chromatography (6% diethyl ether/hexanes, 60 mm silica gel) to give 2-methyl-6-(pentafluorophenyl)aniline as a white powder (0.3 g, 3%). 2-Methyl-3-(pentafluorophenyl)-aniline and 2-methyl-4-(pentafluorophenyl)aniline were also produced; the identity of the desired isomer was confirmed by X-ray crystallography. ^{1}H NMR (300 MHz, $CDCl_3$, 293 K): δ 7.17 (d, $^3J_{HH}$ = 7.4 Hz, 1 H, Ar−*H*), 6.93 (d, $^3J_{HH}$ = 7.4 Hz, 1 H, Ar−*H*), 6.78 (t, $^3J_{HH}$ = 7.4 Hz, 1 H, Ar−*H*), 3.55 (br s, 2 H, N*H*$_2$), 2.23 (s, 3 H, C*H*$_3$). ^{13}C{^{1}H} NMR (75 MHz, $CDCl_3$, 293 K): δ 144.4 (m, Ar *C*-F), 142.8 (s, *C* = N), 140.8 (m, *C*-F), 137.9 (m, Ar *C*-F), 131.8 (t, J_{CF} = 7.5 Hz, *C*CH$_3$), 129.0 (s, Ar *C*-H), 123.2 (s, Ar *C*-H), 118.1 (s, Ar *C*-H), 113.3 (dt, $^2J_{CF}$ = 23 Hz, $^4J_{CF}$ = 7.6 Hz, C_{ipso} of C_6F_5 ring), 110.8 (s, *C*-(C_6F_5)), 17.6 (m, *C*H$_3$). ^{19}F NMR (282 MHz, $CDCl_3$, 293 K): δ −139.0 (dd, $^3J_{FF}$ = 22.1 Hz, $^4J_{FF}$ = 7.9 Hz, 2 F, F_{ortho}), −154.5 (t, $^3J_{FF}$ = 22.1 Hz, 1 F, F_{para}), −161.2 (dt, $^3J_{FF}$ = 22.1 Hz, $^4J_{FF}$ = 7.9 Hz, 2 F, F_{meta}). Anal. Calcd for $C_{13}H_8F_5N$: C, 57.15; H, 2.95; N, 5.13. Found: C, 57.13; H, 2.91; N, 5.11.

Synthesis of (ArN=C(An)−C(An)=NAr) (Ar = 2-Me-6-(C_6F_5)C_6H_3) (1d). To a stirred solution of 2-methyl-6-(pentafluorophenyl)aniline (1.2 g, 4.4 mmol) in 50 mL of methanol were added acenaphthenequinone (0.33 g, 1.8 mmol) and formic acid (0.10 mL, 2.6 mmol). The solution was stirred at room temperature for 48 h, and then the solvent was removed to yield an orange residue. The residue was purified via column chromatography (5% ethyl acetate/hexanes, 60 mm silica gel) to give **1d** as a yellow powder (0.4 g, 32%). An equilibrium between two isomers exists; following chromatography, a 90:10 ratio of isomers is seen, which shifts to a 50:50 ratio after 24 h in $CDCl_3$ at room temperature.

Isomer 1. ^{1}H NMR (300 MHz, $CDCl_3$, 293 K, isomer 1): δ 8.1−6.7 (br m, 12 H, Ar−*H*), 2.03 (s, 6 H, C*H*$_3$). ^{13}C{^{1}H} NMR (75 MHz, $CDCl_3$, 293 K): δ 161.7 (a), 149.1 (h), 146−135 (multiplets for o, p, q), 140.6 (g), 132.1 (f), 130.9 (b), 129.6−129.5 (e and i), 128.5 (d), 127.8 (j), 126.5 (l), 124.1 (k), 122.9 (c), 115.0 (m), 113.9 (t, $^2J_{CF}$ = 15 Hz, n), 17.4 (CH$_3$). ^{19}F NMR (282 MHz, $CDCl_3$, 293 K): δ −136.2 (dd, $^3J_{FF}$ = 22.3 Hz, $^4J_{FF}$ = 7.7 Hz, 2 F, F_{ortho}), −139.0 (dd, $^3J_{FF}$ = 22.3 Hz, $^4J_{FF}$ = 7.7 Hz, 2 F, F_{ortho}), −155.6 (t, $^3J_{FF}$ = 22.3 Hz, 2 F, F_{para}), −162.3 (dt, $^3J_{FF}$ = 22.3 Hz, $^4J_{FF}$ = 7.7 Hz, 2 F, F_{meta}), −163.5 (dt, $^3J_{FF}$ = 22.3 Hz, $^4J_{FF}$ = 7.7 Hz, 2 F, F_{meta}).

Isomer 2: ^{1}H NMR (300 MHz, $CDCl_3$, 293 K): δ 8.1−6.7 (br m, 12 H, Ar−*H*), 2.05 (s, 6 H, C*H*$_3$). ^{13}C{^{1}H} NMR (75 MHz, $CDCl_3$, 293 K): δ 162.5 (a), 149.3 (h), 146−135 (multiplets for o, p, q), 140.9 (g), 132.3 (f), 131.0 (b), 129.6−129.5 (e and i), 128.6 (d), 127.9 (j), 125.9 (l), 124.1 (k), 123.1 (c), 115.6 (m), 113.7 (t, $^2J_{CF}$ = 15 Hz, n), 17.9 (CH$_3$). ^{19}F NMR (282 MHz, $CDCl_3$, 293 K): δ −137.2 (dd, $^3J_{FF}$ = 21.7 Hz, $^4J_{FF}$ = 5.9 Hz, 2 F, F_{ortho}), −139.6 (dd, $^3J_{FF}$ = 22.0 Hz, $^4J_{FF}$ = 6.2 Hz, 2 F, F_{ortho}), −155.0 (broad t, $^3J_{FF}$ = 14.1 Hz, 2 F, F_{para}), −162.9 (broad, 2 F, F_{meta}), −163.3 (broad, 2 F, F_{meta}). Anal. Calcd for $C_{38}H_{18}F_{10}N_2$: C, 65.90; H, 2.62; N, 4.04. Found: C, 65.61; H, 2.58; N, 3.90.

Synthesis of 2. A solution of 2,6-diisopropylaniline (2.66 g, 15.0 mmol) in methanol (20 mL) was added to 1,2-cyclohexanedione (0.73 g, 6.5 mmol). Formic acid (ca. 1 mL) was added to the light yellow solution. After the mixture was stirred for 2 days at room temperature, a white solid precipitated from the red solution and was separated by filtration. The white solid was washed with methanol (3 × 5 mL). NMR analysis indicates the product exists as the imine/enamine tautomer (**2**). Yield of **2** = 1.27 g (45%). ^{1}H NMR (500 MHz, $CDCl_3$, 293 K): δ 7.25−7.05 (m, 6 H, Ar−*H*), 6.43 (s, 1 H, N-*H*), 4.82 (t, *J* = 5 Hz, 1 H, e-*H*), 3.27 (septet, *J* = 7 Hz, 2 H, l or l′), 2.84 (septet, *J* = 6.9 Hz, 2 H, l′ or l), 2.20 (m, 4 H, d and b), 1.74 (quintet, *J* = 5 Hz, 2 H, c), 1.22, 1.20 (2 × d, *J* = 7 Hz, k and *k*′). ^{13}C{^{1}H} NMR (126 MHz, $CDCl_3$, 293 K): δ 162.1 (a), 147.3 (h′), 145.8 (g), 139.6 (f), 137.0 (g′), 136.4 (h), 126.5 (j or j′), 123.4 (i′), 122.9 (i), 106.1 (e), 29.4 (b), 28.4 (l′), 28.3 (l), 24.2 (d), 23.30 (c), 23.25 (*k*′), 22.9 (k). Assignments were made using HMQC and HMBC experiments. Anal. Calcd for $C_{30}H_{42}N_2$: C, 83.67; H, 9.83; N, 6.50. Found: C, 83.32; H, 9.79; N, 6.67.

Synthesis of (ArN=C(Et)−C(Me)=NAr) (Ar = 2,6-C_6H_3-(*i*-Pr)$_2$) (3). A solution of 2,6-diisopropylaniline (4.23 g, 23.9 mmol) in methanol (5.0 mL) was added to 2,3-pentanedione (1.15 g, 11.5 mmol). Formic acid (ca. 0.5 mL) was added to the light yellow solution and the reaction mixture was stirred for several days. The product was isolated using a chromatographic separation on silica gel (0−10% gradient of ethyl acetate in hexanes). The product was a viscous yellow oil which solidified on standing. Yield of **3** = 1.25 g (26%). ^{1}H NMR (500 MHz, $CDCl_3$, 293 K): δ 7.1 (m, 6 H, Ar−*H*), 2.73 (septet, *J* = 6.9 Hz, 4 H, C*H*Me$_2$), 2.56 (q, *J* = 7.6 Hz, 2 H, C*H*$_2$CH$_3$), 2.05 (s, 3 H, C*H*$_3$), 1.23, 1.19, 1.17, 1.14 (all d, *J* = 6.9 Hz, 24 H, CH*Me*$_2$), 1.06 (t, *J* = 7.6 Hz, 3 H, CH$_2$C*H*$_3$). ^{13}C{^{1}H} NMR (126 MHz, $CDCl_3$, 293 K): δ 172.0, 167.8 (2 × *C*=N), 146.2, 145.7 (2 × *ipso*-Ar), 135.2, 135.0 (2 × *ortho*-Ar), 123.7, 123.5 (2 × *para*-Ar), 123.0, 122.8 (2 × *meta*-Ar), 28.4 (*C*H(CH$_3$)$_2$), 23.2 (CH(*C*H$_3$)$_2$), 22.7 (*C*H$_2$CH$_3$) 22.2 (CH(*C*H$_3$)$_2$), 17.2 (CH$_3$), 10.6 (CH$_2$). Assignments were made using an HMQC experiment. Anal. Calcd for $C_{29}H_{42}N_2$: C, 83.20; H, 10.11; N, 6.69. Found: C, 83.24; H, 10.11; N, 6.67.

Synthesis of (ArN=C(An)−C(An)=NAr)NiBr$_2$ (Ar = 2-$CF_3C_6H_4$) (4a). (DME)$NiBr_2$ (111 mg, 0.36 mmol) and **1a** (187 mg, 0.40 mmol) were combined in a Schlenk flask under an argon atmosphere. CH_2Cl_2 (20 mL) was added, and the reaction stirred at room temperature for 18 h. The supernatant liquid was removed, and the product washed with 2 × 10 mL of Et_2O and dried in vacuo. The product was isolated as a red-brown powder (220 mg, 89% yield).

Synthesis of (ArN=C(An)−C(An)=NAr)NiBr$_2$ (Ar = 2-Me-6-$CF_3C_6H_3$) (4b). Following the above procedure, **4b** was isolated as a red powder in 94% yield.

Synthesis of (ArN=C(An)−C(An)=NAr)NiBr$_2$ (Ar = 2-(C_6F_5)C_6H_4) (4c). Following the above procedure, **4c** was isolated as a yellow powder (0.3 g, 42% yield). Crystals suitable for an X-ray diffraction experiment were obtained by slow diffusion of pentane into a saturated dichloromethane solution of **4c**. Anal. Calcd for $C_{36}H_{14}Br_2F_{10}N_2Ni$: C, 48.97; H, 1.60; N, 3.17. Found: C, 48.77; H, 1.64; N, 3.08.

Synthesis of (ArN=C(An)−C(An)=NAr)NiBr$_2$ (Ar = 2-Me-6-(C_6F_5)C_6H_3) (4d). Following the above procedure, **4d** was isolated as an orange powder (0.25 g, 42% yield). Crystals suitable for an X-ray diffraction experiment were obtained by slow diffusion of pentane into a saturated dichloromethane solution of **4d**. Anal. Calcd for $C_{38}H_{18}Br_2F_{10}N_2Ni$: C, 50.10; H, 1.99; N, 3.07. Found: C, 49.88; H, 1.94; N, 3.03.

Synthesis of (ArN=C(CH$_2$CH$_2$CH$_2$CH$_2$)C=NAr)NiBr$_2$ (Ar = 2,6-C_6H_3(*i*-Pr)$_2$) (5). Following the above procedure, **5** was isolated as a red powder in 48% yield.

Synthesis of (ArN=C(Et)−C(Me)=NAr)NiBr$_2$ (Ar = 2,6-C_6H_3(*i*-Pr)$_2$) (6). Following the above procedure, **6** was isolated as a red powder in 84% yield.

General Procedure for 1 atm Polymerizations. Toluene (100 or 200 mL) was added to a flask under 1 atm of ethylene pressure at the desired temperature (regulated by a water bath). MMAO (1.6 mL; Al:Ni = 1000−3000) was added to the stirred solution, and the temperature was allowed to equilibrate for 10−15 min. The appropriate Ni(II) complex was dissolved/suspended in 5 mL of toluene and was rapidly added to the reaction mixture. The polymerization mixture was stirred for 20 or 30 min under 1 atm of ethylene then was quenched by addition of methanol, acetone, and ca. 5 mL of 6 M HCl. Polyethylene precipitated from solution, and was isolated by removal of the solvents and dried in vacuo. For the 85 °C runs, the polymer did not precipitate from the

Table 8. X-ray Crystallographic Data for 4c and 4d

	4c	4d
formula	$NiBr_2C_{36}H_{18}F_{10}N_2O_2 \bullet (1/3)H_2O$	$NiBr_2C_{38}H_{18}F_{10}N_2$
FW	925.05	911.07
cryst class	triclinic	monoclinic
space group		*P*2/*c*
color	yellow	orange
a (Å)	14.3043(6)	17.3143(8)
b (Å)	15.0408(6)	11.3596(5)
c (Å)	25.9407(11)	19.8097(9)
α (deg)	96.9580(10)	
β (deg)	105.2400(10)	113.3180(10)
γ (deg)	107.5340(10)	
V (Å^3)	5011.4(4)	3578.0(3)
Z	6	4
D(calc) (g cm^{-3})	1.839	1.691
R_F [$I > 3\sigma(I)$]	0.047	0.060
R_w (all data)	0.050	0.074
GoF	2.01	1.96

[a] Definition of *R* indices: $R_F = \sum(F_o - F_c)/\sum(F_o)$; $R_w = [\sum[w(F_o - F_c)^2]/\sum[w(F_o)^2]]^{1/2}$.

quenched reaction mixture, and had to be isolated by solvent evaporation on a rotary evaporator, followed by washing with HCl (6 M), methanol, and acetone and drying in vacuo.

General Procedure for High-Pressure Polymerizations. A 1000 mL Parr autoclave was heated under vacuum at 60 °C for several hours and then was cooled and backfilled with ethylene. Toluene (200 mL) and MMAO (1.6 mL; Al:Ni = 1000−3000) were added, the autoclave sealed, and the ethylene pressure raised to ca. 50 psig. The reaction temperature was established and the mixture allowed to stir for 15 min. The autoclave was then vented, the precatalyst solution/suspension added, and the autoclave sealed and pressurized to the desired ethylene pressure while stirring. For 35 °C runs the temperature was maintained by cooling with an ice/water cooled circulator. The reaction was quenched by venting the autoclave followed by addition of methanol or acetone. The precipitated polymers were filtered from solution and dried in vacuo.

Ethylene Flow Rate Measurements. A mechanically stirred 1000 mL Parr autoclave under an ethylene atmosphere was charged with 198 mL of toluene and MMAO. The reactor was sealed and pressurized with ethylene to 200 psig, and the temperature was allowed to equilibrate at the reaction temperature. Once the system reached equilibrium, the ethylene flow baseline was established with a mass flowmeter positioned between the ethylene supply cylinder and the autoclave. The reactor was vented, and a suspension of **4c** (0.6 mg, 7 × 10^{-7} mol) in toluene (2 mL) was transferred into the reactor via cannula. The reactor was repressurized to 200 psig with ethylene, and the temperature maintained within 1 °C of the desired reaction temperature. Ethylene flow rates were recorded at 5−15 s intervals throughout the duration of the reaction.

Crystallographic Structural Determinations. Crystals of **4c** and **4d** suitable for X-ray crystallography were grown at room temperature from a saturated CH_2Cl_2 solution with slow diffusion of diethyl ether. Single crystals were mounted in oil on the end of a fiber. Intensity data were collected on a Bruker SMART 1K diffractometer with CCD detector using Mo Kα radiation of wavelength 0.710 73 Å using 0.3° *ω* corrected intensity data. The structures were solved by direct methods and refined by least squares techniques using the NRCVAX[57] suite of programs. All non-hydrogen atoms were refined to ride on the atoms to which they were bonded. Crystal data, data collection, and refinement parameters[58] are listed in Table 8.

Acknowledgment. This work was supported by the National Science Foundation and DuPont. S.A.S. thanks the United States Air Force Institute of Technology Civilian Institutions program (AFIT/CI) for sponsorship. E.O. acknowledges the Spanish Ministry of Education and Culture for support. D.P.G. gratefully acknowledges the Natural Sciences and Engineering Research Council (NSERC) of Canada for a Postdoctoral Fellowship. We would also like to thank Scott Shultz for assistance with the DSC analysis, Steve Gross and Dr. Bill Sichina for assistance with the DMA experiment, Dan Tempel for assistance with the synthesis of **6**, and the DuPont analytical group for conducting the high temperature GPC analyses.

References and Notes

(1) See for example: (a) Brintzinger, H. H.; Fischer, D.; Mülhaupt, R.; Rieger, B.; Waymouth. R. M. *Angew. Chem., Int. Ed. Engl.* **1995**, *34*, 1143. (b) McKnight, A. L.; Waymouth, R. M. *Chem. Rev.* **1998**, *98*, 2587. (c) Yang, X.; Stern, C. L.; Marks, T. J. *J. Am. Chem. Soc.* **1994**, *116*, 10015. (d) Britovsek, G. J. P.; Gibson, V. C.; Wass, D. F. *Angew. Chem., Int. Ed. Engl.* **1999**, *38*, 429. (e) Bochmann, M. *J. Chem. Soc., Dalton Trans.* **1996**, 255. (f) Fink, G.; Mülhaupt, R.; Brintzinger, H. H., Eds. *Ziegler Catalysts: Recent Scientific Innovations and Technological Improvement*; Springer-Verlag: Berlin, 1995.

(2) Schmidt, G. F.; Brookhart, M. *J. Am. Chem. Soc.* **1985**, *107*, 1443.

(3) Brookhart, M.; Volpe, A. F.; Lincoln, D. M.; Horvath, I. T.; Millar, J. M. *J. Am. Chem. Soc.* **1990**, *112*, 5634.

(4) Brookhart, M.; DeSimone, J. M.; Grant, B. E.; Tanner, M. J. *Macromolecules* **1995**, *28*, 5378.

(5) Wang, L.; Flood, T. C. *J. Am. Chem. Soc.* **1992**, *114*, 3169.

(6) Timonen, S.; Pakkanen, T. T.; Pakkanen, T. A. *J. Mol. Catal.* **1996**, *111*, 267.

(7) For early examples of Ni-catalyzed ethylene polymerization see: (a) Keim, W.; Appel, R.; Storeck, A.; Krüger, C.; Goddard, R.; *Angew. Chem., Int. Ed. Engl.* **1981**, *20*, 116. (b) Klabunde, U.; Ittel, S. D. *J. Mol. Catal.***1987**, 123. (c) Klabunde, U.; Mülhaupt, R.; Herskovitz, T.; Janowicz, A. H.; Calabrese, J.; Ittel, S. D. *J. Polym. Sci., Part A: Polym. Chem.* **1987**, *25*, 1989. (c) Ostoja Starzewski, K. A.; Witte, J. *Angew. Chem., Int. Ed. Engl.* **1987**, *26*, 63.

(8) Johnson, L. K.; Killian, C. M.; Brookhart, M. *J. Am. Chem. Soc.* **1995**, *117*, 6414. Following initial discoveries at UNC, collaborative efforts were initiated with the group at DuPont.

(9) (a) Johnson, L. K.; Killian, C. M.; Arthur, S. D.; Feldman, J.; McCord, E. F.; McLain, S. J.; Kreutzer, K. A.; Bennett, A. M. A.; Coughlin, E. B.; Ittel, S. D.; Parthasarathy, A.; Tempel, D. J.; Brookhart, M. S. WO 96/23010. (b) Brookhart, M. S.; Johnson, L. K.; Arthur, S. D.; Feldman, J.; Kreutzer, K. A.; Bennett, A. M. A.; Coughlin, E. B.; Ittel, S. D.; Parthasarathy, A.; Tempel, D. J. U.S. Patent 5 886 224, 1999. (c) Brookhart, M. S.; Johnson, L. K.; Killian, C. M.; Arthur, S. D.; Feldman, J.; McCord, E. F.; McLain, S. J.; Kreutzer, K. A.; Bennett, A. M. A.; Coughlin, E. B.; Ittel, S. D.; Parthasarathy, A.; Wang, L.; Yang, Z. U.S. Patent 5 866 663, 1999. (d) Brookhart, M. S.; Johnson, L. K.; Killian, C. M.; Arthur, S. D.; McCord, E. F.; McLain, S. J. U.S. Patent 5 891 963. (e) Brookhart, M. S.; Johnson, L. K.; Killian, C. M.; McCord, E. F.; McLain, S.

J.; Kreutzer, K. A.; Ittel, S. D.; Tempel, D. J. U.S. Patent 5 880 241, 1999.
(10) Killian, C. M.; Tempel, D. J.; Johnson, L. K.; Brookhart, M. *J. Am. Chem. Soc.* **1996**, *118*, 11664.
(11) Killian, C. M.; Johnson, L. K.; Brookhart, M. *Organometallics* **1997**, *16*, 2005.
(12) Svejda, S. A.; Brookhart, M. *Organometallics* **1999**, *18*, 65.
(13) McLain, S. J.; Feldman, J.; McCord, E. F.; Gardner, K. H.; Teasley, M. F.; Coughlin, E. B.; Sweetman, K. J.; Johnson, L. K.; Brookhart, M. *Macromolecules* **1998**, *31*, 6705.
(14) Möhring, V. M.; Fink, G. *Angew. Chem., Int. Ed. Engl.* **1985**, *24*, 1001.
(15) Schubbe, R.; Angermund, K.; Fink, G.; Goddard, R. *Macromol. Chem. Phys.* **1995**, *196*, 467.
(16) Feldman, J.; McLain, S. J.; Parthasarathy, A.; Marshall, J.; Calabrese, J. C.; Arthur, S. D. *Organometallics* **1997**, *16*, 1514.
(17) Schleis, T.; Spaniol, T. P.; Okuda, J.; Heinemann, J.; Mülhaupt, R. *J. Organomet. Chem.* **1998**, *569*, 159.
(18) Wang, C.; Friedrich, S.; Younkin, T. R.; Li, R. T.; Grubbs, R. H.; Bansleben, D. A.; Day, M. W. *Organometallics* **1998**, *17*, 3149.
(19) Pellecchia, C.; Zambelli, A. *Macromol. Rapid. Commun.* **1996**, *17*, 333.
(20) Pappalardo, D.; Mazzeo, M.; Pelleccia, C. *Macromol. Rapid. Commun.* **1997**, *18*, 1017.
(21) Pelleccia, C.; Zambelli, A.; Mazzeo, M.; Pappalardo, D. *J. Mol. Catal. (A)* **1998**, *128*, 229.
(22) Galland, G. B.; de Souza, R. F.; Mauler, R. S.; Nunes, F. F. *Macromolecules* **1999**, *32*, 1620.
(23) Zeng, X.; Zetterberg, K. *Macromol. Chem. Phys.* **1998**, *199*, 2677.
(24) Kim, J. S.; Pawlow, J. H.; Wojcinski, L. M.; Murtuza, S.; Kacker, S.; Sen, A. *J. Am. Chem. Soc.* **1998**, *120*, 1932.
(25) Johnson, L. K.; Mecking, S.; Brookhart, M. *J. Am. Chem. Soc.* **1996**, *118*, 267.
(26) Mecking, S.; Johnson, L. K.; Wang, L.; Brookhart, M. *J. Am. Chem. Soc.* **1998**, *120*, 888.
(27) Small, B. L.; Brookhart, M.; Bennett, A. M. A. *J. Am. Chem. Soc.* **1998**, *120*, 4049.
(28) Britovsek, G. J. P.; Gibson, V. C.; Kimberly, B. S.; Maddox, P. J.; McTavish, S. J.; Solan, G. A.; White, A. J. P.; Williams, D. J. *Chem. Commun.* **1998**, 849.
(29) (a) Small, B. L.; Brookhart, M. *Macromolecules* **1999**, *32*, 2120. (b) Pellecchia, C.; Mazzeo, M.; Pappalardo, D. *Macromol. Rapid. Commun.* **1998**, *19*, 651.
(30) 1,3-Enchainment in polymerizations of cyclopentene has previously been observed for early metal metallocene catalysts. See: Collins, S.; Kelly, W. M. *Macromolecules* **1992**, *25*, 233. Kelly, W. M.; Taylor, N. J.; Collins, S. *Macromolecules* **1994**, *27*, 4477. Kelly, W. M.; Wang, S.; Collins, S. *Macromolecules* **1997**, *30*, 3151.
(31) Tempel, D. J.; Brookhart, M. *Organometallics* **1998**, *17*, 2290.
(32) Svejda, S. A.; Johnson, L. K.; Brookhart, M. *J. Am. Chem. Soc.* **1999**, *121*, 10634.
(33) ^{13}C NMR spectroscopic and light scattering studies have shown that the polyethylene produced with (α-diimine)-palladium(II) catalysts is hyperbranched. See ref 9 and: Guan, Z.; Cotts, P. M.; McCord, E. F.; McLain, S. J. *Science* **1999**, *283*, 2059.
(34) Deng, L.; Margl, P.; Ziegler, T. *J. Am. Chem. Soc.* **1997**, *119*, 1094.
(35) Deng, L.; Woo, T. K.; Cavello, L.; Margl, P. M.; Ziegler, T. *J. Am. Chem. Soc.* **1997**, *119*, 6177.
(36) Musaev, D. G.; Froese, R. D. J.; Morokuma, K. *Organometallics* **1998**, *17*, 1850.
(37) Froese, R. D. J.; Musaev, D. G.; Morokuma, K. *J. Am. Chem. Soc.* **1998**, *120*, 1581.
(38) van Asselt, R.; Elsevier: C. J.; Smeets, W. J. J.; Spek, A. L.; Benedix, R. *Recl. Trav. Chim. Pays-Bas* **1994**, *113*, 88.
(39) tom Dieck, H.; Svoboda, M.; Grieser, T. *Z. Naturforsch.* **1981**, *36b*, 823.
(40) Due to the high activity of these catalysts, even under conditions of high dilution and low catalyst loadings, the consumption of monomer is very rapid, and the catalyst rapidly becomes starved for monomer.
(41) Turnover frequency (TOF) is calculated as the moles of ethylene consumed per mole of catalyst used per unit of time (h).
(42) It is also possible that the 2,6-disubstituted aryl groups undergo slow rotation in solution, however on the time scale of the polymerization reactions, it is likely that these groups are fixed either in the C_2 or C_s conformations.
(43) Turnover frequencies given assume complete catalyst activation. Recent results suggest initial reaction with methylaluminoxane may produce some inactive nickel materials: Gates, D. P.; Brookhart, M. Unpublished results.
(44) Killian, C. M. Ph.D. Thesis, University of North Carolina at Chapel Hill, 1996.
(45) The branching numbers determined by ^{1}H NMR give no information about the types of branches (i.e., methyl, ethyl, propyl), A series of multidimensional NMR experiments conducted by E. M. McCord on polyethylene produced from nickel diimine catalysts indicate the frequency of branching to be Me > Et > Pr > Bu, etc. See ref 9.
(46) Activation of an *ortho* C−H bond in a (DAD)$NiBr_2$ compound [DAD = glyoxalbis(diisopropylmethylimine)] has been observed in reactions with bulky *o*-tolylmagnesium bromide. See: tom Dieck, H.; Svoboda, M. *Chem. Ber.* **1976**, *109*, 1657. We have also observed an intramolecular C−H activation in (2,6-diisopropyl)phenyl-substituted [(α-diimine)Pd(Me)OEt_2]$^+$ complexes in solution: Johnson, L. K.; Tempel, D. J.; Brookhart, M. Unpublished results.
(47) Monomer flow measurements using ortho alkyl-substituted catalysts (**4f**) was attempted for comparative purposes; however, the data were unreliable because the polyethylene formed is not very soluble in the reaction solution. The reaction mixture becomes heterogeneous in less than 30 min and thus long-term flow data are inconsistent.
(48) The melt transitions reported in Tables 1−5 are peak T_m's. Due to the differences in the types of branching present in polyethylenes produced with different catalysts and under different conditions, the shapes of the melt transitions vary from very sharp for highly linear polymers to very broad ill-defined endotherms for highly branched samples. In all cases for consistency we have reported, as T_m, the temperature of the transition at peak maximum. It is very difficult to compare the branching numbers with the reported peak T_m's without also considering (i) the type of branching present and (ii) the shape of the melt endotherm. For example in Table 3 (entries 23 and 24), polymers prepared with catalyst **6** at 400 and 600 psig, respectively, show similar T_m's and branching numbers but inspection of the DSC thermograms show that the shapes of the melt transitions are quite different (entry 23 being much broader than entry 24). It becomes even more difficult to quantitatively compare branching vs T_m for polymers prepared using different catalysts. For example, catalyst **4f** at 200 and 400 psig (35 °C) yields polymers with 13 and 12 branches respectively (Table 3 entries 13 and 14) and catalyst **5** at 400 and 600 psig (35 °C) yields polymers with 11 branches (Table 5, entries 20 and 21), yet despite similar branching numbers, T_m's are 128 and 126 °C for polymers from catalyst **4f** and 108 and 114 °C for polymers from catalyst **5**. Of course, the shapes of the melt curves are remarkably different. What is clear from the data is that, in general, the larger the branching number the lower the T_m and that the properties of the polyethylenes produced are highly sensitive to both the nature of the catalyst and the conditions under which the polymerizations are carried out.
(49) Doak, K. W. In *Encyclopedia of Polymer Science and Engineering*, revised ed.; Mark, H. F., Kroschwitz, J. I., Eds.; Wiley-Interscience: New York, 1986; Vol. 6; see p 410.
(50) Hoffman, J. D.; Williams, G.; Passaglia, E. *J. Polym. Sci.: Part C* **1966**, *14*, 173.
(51) Popli, R.; Glotin, M.; Mandelkern, L.; Benson, R. S. *J. Polym. Sci.: Polymer Phys.* **1984**, *22*, 407.
(52) Alberola, N.; Cavaille, J. Y.; Perez, J. *Eur. Polym. J.* **1992**, *28*, 935.
(53) Pangborn, A. B.; Ciardello, M. A.; Grubbs, R. H.; Rosen, H. K.; Timmers, F. J. *Organometallics* **1996**, *15*, 1518.
(54) Svoboda, M.; tom Dieck, H. *J. Organomet. Chem.* **1980**, *191*, 321.
(55) Chen, Q. Y.; Li, Z. T. *J. Org. Chem.* **1993**, *58*, 2599.
(56) Chupp, J. P.; Balthazor, T. M.; Miller, M. J.; Pozzo, M. J. *J. Org. Chem.* **1984**, *49*, 4711.
(57) Gabe, E. J.; LePage, Y.; Charland, J. P.; Lee, F. L.; White, P. S. *J. Appl. Crystallogr.* **1989**, *22*, 284.
(58) Full details of the determination of the X-ray crystal structures of **4c** and **4d** have been deposited with the Cambridge Crystallographic Centre. The coordinates can be obtained, on request, from the Director, Cambridge Crystallographic Data Centre, 12 Union Road, Cambridge CB2 1EZ, U.K. (CCDC129234 and CCDC129234, respectively).

MA991234+